



JRC TECHNICAL REPORTS

Cold atom interferometry sensors: physics and technologies

*A scientific background
for EU policymaking*

Travagnin, M.

2020

This publication is a Technical report by the Joint Research Centre (JRC), the European Commission's science and knowledge service. It aims to provide evidence-based scientific support to the European policymaking process. The scientific output expressed does not imply a policy position of the European Commission. Neither the European Commission nor any person acting on behalf of the Commission is responsible for the use that might be made of this publication.

Contact information

Name: Martino Travagnin
Email: Martino.Travagnin@ec.europa.eu

EU Science Hub

<https://ec.europa.eu/jrc>

JRC121223

EUR 30289 EN

PDF ISBN 978-92-76-20405-3 ISSN 1831-9424 doi:10.2760/315209

Luxembourg: Publications Office of the European Union, 2020

© European Union, 2020

The reuse policy of the European Commission is implemented by Commission Decision 2011/833/EU of 12 December 2011 on the reuse of Commission documents (OJ L 330, 14.12.2011, p. 39). Reuse is authorised, provided the source of the document is acknowledged and its original meaning or message is not distorted. The European Commission shall not be liable for any consequence stemming from the reuse. For any use or reproduction of photos or other material that is not owned by the EU, permission must be sought directly from the copyright holders.

All content © European Union, 2020

How to cite this report:

M. Travagnin, *Cold atom interferometry sensors: physics and technologies. A scientific background for EU policymaking*, 2020, EUR 30289 EN, Publications Office of the European Union, Luxembourg, 2020, ISBN 978-92-76-20405-3, doi:10.2760/315209, JRC121223

Contents

Acknowledgements 1

Abstract 2

1 Introduction 3

2 Underlying physics 6

3 Research highlights 14

 3.1 Gyroscopes and accelerometers 14

 3.2 Gravimeters and gravity gradiometers 25

4 Worldwide players 36

5 Conclusions 39

References 40

List of abbreviations and definitions 42

Acknowledgements

This work has been done in the framework of the SynQArc administrative arrangement between DG JRC and DG DEFIS. I am glad to acknowledge continuous help from my JRC colleague Adam Lewis, and useful conversations with several DG DEFIS colleagues.

Abstract

This report describes the physical principles underpinning cold atom interferometry (CAI) and shows how they can be leveraged to develop high-performance inertial and gravity sensors; the distinguishing properties and the maturity level of such sensors will also be assessed.

Proof-of-principles demonstrations have been made for CAI-based accelerometers and gyroscopes, which can enable long-term autonomous navigation and precise positioning for ships, submarines, and satellites. CAI-based gravimeters and gravity gradiometers have been developed and are being tested on the ground; satellite-based systems could in the future be used to monitor the Earth gravity field. This would allow a better understanding of several geophysical and climate phenomena which require long-term policies solidly supported by data.

Quantum sensors based on cold atom interferometry may therefore impact existing and future EU programmes on space, defence, and Earth observation. This report provides background knowledge of the field to a non-specialist audience, and in particular to EU policymakers involved in technology support and potential applications.

1 Introduction

It is well-known that the quantum properties of atoms can be exploited for a number of important applications, such as measuring time and frequency, storing and processing information, and sensing. Since their implementation typically requires the atoms to interact with one or more laser beams, the atoms must remain confined in a region of space where they can be shone upon by the beams in charge of quantum state initialization, manipulation, and interrogation. In sensors, the manipulation step corresponds to the interaction with the operator representing the quantity to be measured. Since the atoms must remain in the laser beam paths all the time necessary for the required interactions to take place, the need to reduce their thermal motion arises.

An atom can therefore be considered to be “cold” when its thermal velocity has been reduced to such an extent that it becomes possible to interact with it in a manner that makes its quantum properties accessible and exploitable. In more technical terms, the atomic wavefunction which represents the probability density must remain confined for a long enough time in the volume where the required light-matter interactions take place. This aim is usually accomplished by combining the trapping potential generated by a magnetic field with three pairs of suitably crafted counter-propagating laser beams, which repeatedly interact with the atom in such a way to progressively reduce its momentum. The whole device goes under the name of magneto-optical trap (MOT). Laser systems therefore play a fundamental role in cold atom physics, since they first cool the atom and then they interact with it by sequentially changing its quantum state according to the requirements of the targeted application. The atoms emerging from a MOT have typical temperatures in the micro-Kelvin ($1\mu\text{K} = 10^{-6}$ Kelvin) range. Each of them then undergoes a sequence of interactions with the laser beams orchestrating the application, which ends with a measurement of the final quantum state. Since each atom behaves independently from the others, the total system response will be given by an incoherent superposition of signals. The shot noise amplitude affecting the system will therefore decrease as $1/N^{1/2}$, N being the number of atoms which undergo all the required interaction steps.

There exists however a completely different state of matter, called a Bose-Einstein condensate (BEC), for which atoms must be cooled down to the nano-Kelvin ($1\text{nK} = 10^{-9}$ Kelvin) range. Under suitably controlled conditions, at these ultra-cold temperatures the atoms cannot be described by independent wavefunctions: the whole atomic system coalesces in a sort of macroscopic quantum state which is described by a unique wavefunction. To reach the temperatures necessary for the atoms to condense in the Bose-Einstein state a MOT does not suffice, and after having emerged from it the atoms must undergo further cooling processes. Since a BEC is described by a single wavefunction, all of its atoms behave coherently: the overall system response will thus not be affected by shot noise. This constitutes a very interesting feature, in particular for applications requiring very high sensitivity levels. Generally speaking, BECs have not yet reached the technological maturity required for field applications: most of the research is still focused on understanding the properties of the condensate itself, and identifying the main factors which cause the observed experimental deviations in the phenomenon from the theoretical predictions. It must however be acknowledged that the last ~ 20 years have seen a remarkable interest in the use of BECs for scientific experiments aimed at tests of fundamental physical theories.

The history of the technical developments which enabled the trapping of atoms and the interaction with atomic systems can be traced by mentioning the related Nobel Prizes in Physics: in 1989 “for the development of the ion trap technique”, in 1997 “for the development of methods to cool and trap atoms with laser light”, and in 2012 “for ground-breaking experimental methods that enable measuring and manipulation of individual quantum systems”. In 2001 the Nobel Prize in Physics was awarded “for the

achievement of Bose-Einstein condensation in dilute gases of alkali atoms, and for early fundamental studies of the properties of the condensates."

Cold atom interferometry represents a peculiar way to exploit cold atoms, since it leverages both the amplitude and the phase of the atomic wavefunction. Sensors based on cold atom interferometry require an accurate measurement of the phase difference which accumulates as the atom travels along the two arms of an interferometer. At the interferometer entrance the atomic wavefunction is split in two components which travel along two different paths; inside the interferometer they build up a phase difference which depends on the magnitude of the effect we are interested in, and which can be measured at the interferometer output. Since inertial or gravitational effects affect the phase difference, the interferometer represents an accurate inertial probe: gravimeters, gravity gradiometers, accelerometers and gyroscopes can therefore be built on this working principle¹. As a scientific discipline, matter-wave interferometry is several decades old, and thanks to recent progress in cold atoms technologies it is now delivering its first commercial products. Fig. 1 tries to capture in a synthetic way the evolution of CAI-based inertial sensing.

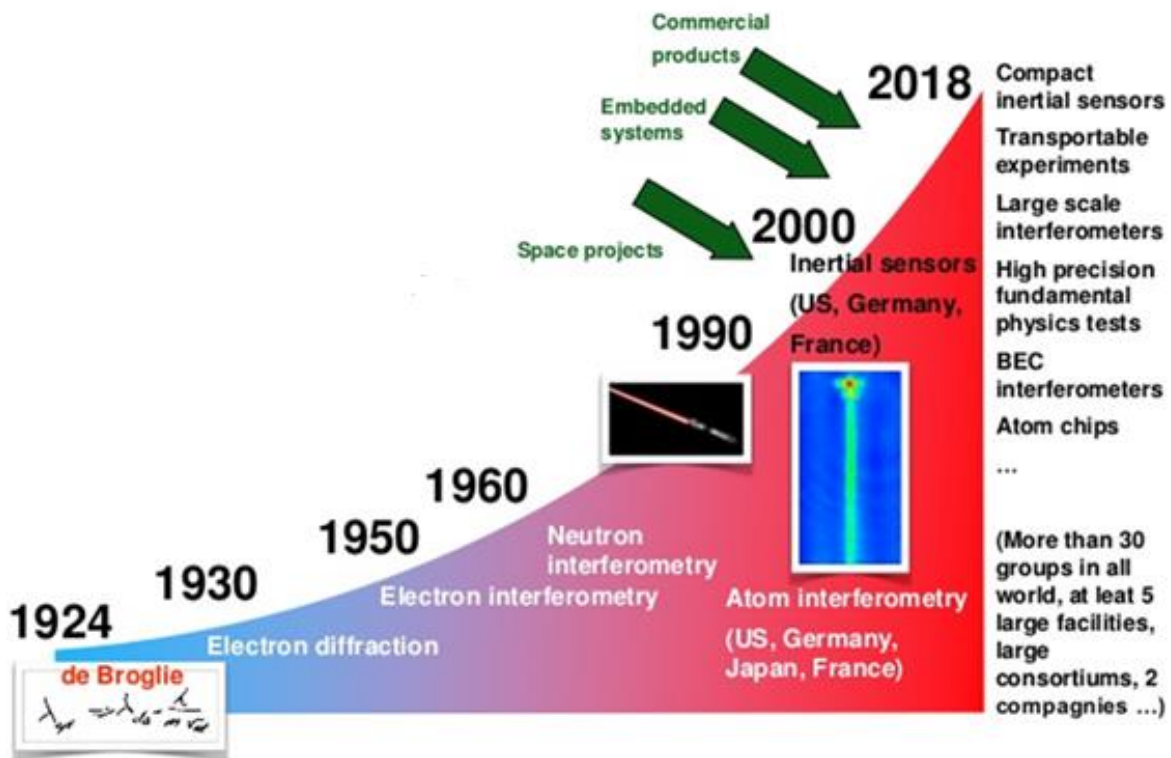


Fig. 1: A timeline of cold atom interferometry for sensing applications².

The fundamental argument that triggered the development of CAI-based sensors is that an atomic interferometer can, in principle, have sensitivity several orders of magnitude higher than that of an optical one with similar dimensions. Indeed, its sensitivity increases with the square of the interrogation time, i.e. the time spent by the atom inside the interferometer. A second important argument is that in CAI-based inertial sensors the only moving parts are atoms, whose inertial properties are guaranteed to remain unaltered over time. This should provide a better long-term stability with respect to

¹ "Mobile and remote inertial sensing with atom interferometers", B. Barrett et al., Proceedings of the International School of Physics 'Enrico Fermi', 188, 493-555, 2014; <https://arxiv.org/pdf/1311.7033.pdf>

² "Experimental gravitation and geophysics with matter wave sensors", P. Bouyer, Frontier of matter-wave optics conference, 2018; <https://www.matterwaveoptics.eu/FOMO2018/school/lecture-notes/Bouyer%20-%20experimental%20gravitation%20and%20geophysics%20with%20matterwave%20sensors.pdf>

sensors based on the movement of macroscopic systems whose dynamical properties change because of the unavoidable use-induced wear and tear, thus causing in their measurements a drift that must be counteracted by frequent recalibrations. A third property which compares favourably with respect to several competing techniques is that CAI-based inertial sensors provide an absolute measure of the quantity being targeted, and not an evaluation of its variation with respect to a reference value. Because of these characteristics, sensors based on cold atom interferometry offer relevant advantages for accelerometers, gyroscopes, gravimeters and gravity gradiometers to be used for inertial guidance, geoid determinations, geophysics and metrology. CAIs are also excellent candidates for tests of general relativity and for the detection of gravitational waves, especially if the microgravity environment of a satellite allows increasing the sensitivity by allowing longer interrogation times.

It must however be acknowledged that at the present development level the advantages of a CAI-based sensor come at the price of high cost, size, weight, and power footprint, since leveraging the physical working principles of cold atom interferometry require complex advanced technologies (vacuum systems, lasers and optical systems, control electronics, etc.). Progress in enabling technologies constitutes therefore a key factor for the development of field-deployable inertial sensors. It is also likely that the first use-cases for CAI inertial sensors will be found in very specialized high-end applications, which can tolerate the high development cost of a custom solution. In this regard space and defence programs, which are typically backed by long term policies sensitive to strategic autonomy concerns, represent a credible arena where to look for applications.

The report focuses on CAI embodiments which have reached a technological maturity level which suggests possible fruition in the next ~ 10 years. Typical dimensions of devices are in the meter scale, with atoms temperatures in the μK range. Chip-scale devices (typically with $\sim \text{cm}$ sizes) and Bose-Einstein condensates ($\sim \text{nK}$ temperatures) will be addressed more tangentially, since they can generally be considered to be at an earlier development stage. Indeed, researchers working on atomic chip interferometers and on BEC interferometry are proceeding along very different paths and investigating an incredible variety of solutions, whose description transcends the scope of this report; some examples will nevertheless be presented. For completeness, we will also give some coverage to applications of CAI for fundamental physics experiments (e.g. gravitational wave detection, tests of general gravity): although they typically have aims and requirements very different from those of the applications we are here analysing, they can constitute a significant technology development driver.

The material of the report is organized as follow: in Section 2 we the physics underlying CAI inertial sensors will be presented, in Section 3 we will highlight some technologies and describe actual devices being developed, and in Section 4 we will provide a list of the main players in the field. Section 5 will present the main conclusions of the report.

2 Underlying physics

As a preliminary note, we warn the reader that the present description is intended only to provide an essential background on the physics underlying the principles of cold atom interferometry. Although the approach described here is rather common, several others are being explored; in addition, the technical details of the actual embodiments vary very much in the different implementations which have been presented to the scientific community. This state of play follows from the variety of the aims being pursued, but it also indicates that a unique consolidated technique has yet to emerge, as it is typical for systems having a still relatively low technological maturity level. An atomic interferometer requires manipulating atomic wavefunctions, which can be acted upon in several different ways: indeed, depending on its specific state, an atom can be affected by its interaction with laser beams, radio frequency pulses, magnetic fields, etc. The choice of how to operate on an atomic wavefunction depends on the aims and the convenience of the experimenter: in this description we will show the approach most commonly taken for laboratory-scale and portable CAI sensors, which heavily relies on lasers both to cool the atoms to the μK range and to manipulate their states. In chip-scale devices magnetic fields and RF pulses are more commonly employed, respectively to guide the atoms along the chip and to change their state³. Interferometers based on Bose-Einstein condensates, where atoms are cooled to $\sim\text{n}^\circ\text{K}$, are less technologically mature and will not be covered in this excursus.

A general conceptual scheme of an atomic interferometer is shown in Fig. 2. A source generates a cloud of cold atoms, which then interacts with a laser beam that filters out all those which are not in a suitable initial ground state. The remaining atoms enter the interferometer proper, which is implemented by a succession of three laser pulses. The system is designed in such a way that each atom exits from the interferometer with a certain probability of having transitioned to an excited state, and this probability depends on the signal to be measured. The atomic cloud is therefore split by the interferometer in two spatially separated parts, one composed of atoms in the initial ground state and the other of atoms in the excited state. A detection stage, usually relying on laser induced fluorescence, quantifies the relative populations of the two clouds exiting the interferometer: the relative population is determined by the transition probability, and therefore provides a measurement of the signal we are interested in.

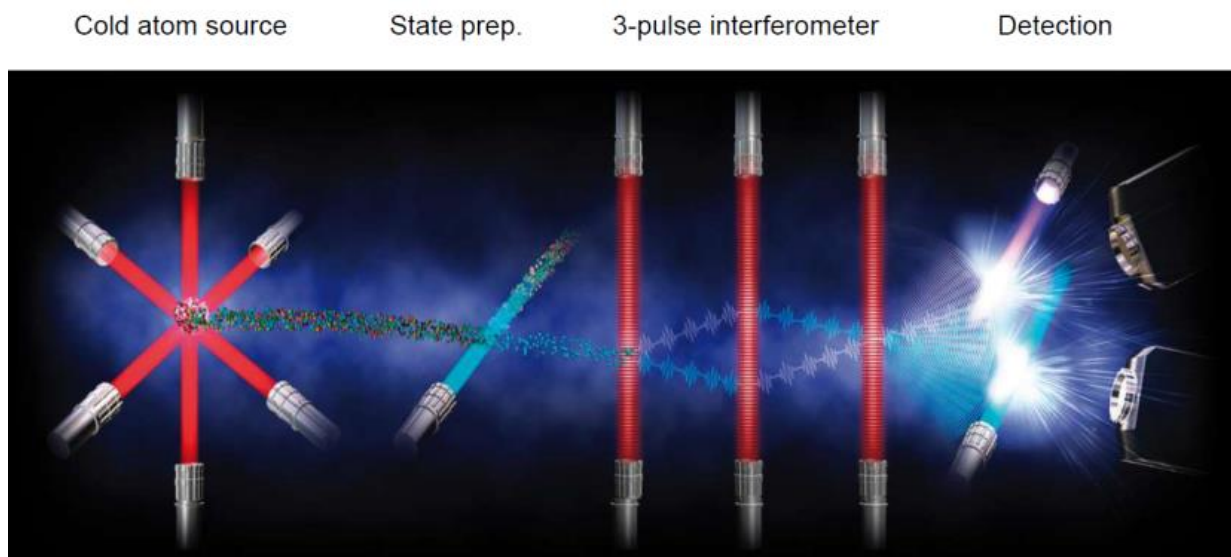


Fig. 2: Conceptual scheme of a cold atom interferometer. The pulses are separated by a time interval T , so the total permanence time of the atomic cloud inside the interferometer is $2T$.

³ "Fifteen years of cold matter on the atom chip: promise, realizations, and prospects", Mark Keil et al., Journal of Modern Optics, Vol. 63, N. 18, 1840-1885, 2016; <https://doi.org/10.1080/09500340.2016.1178820>

Fig. 3 shows the working principles of a typical cold atom source, which consists of a magneto-optical trap formed by two coils which generate the magnetic field used to confine the atoms, and three pairs of counter-propagating laser beams which cool the atoms down to the $\mu^\circ\text{K}$ range. Atomic species particularly suited to undergo this process are alkali metals such as ^{39}K , ^{87}Rb (the workhorse) and ^{133}Cs . From the right-hand figure we also see that an atomic ensemble cooled to $2\mu^\circ\text{K}$ would reach, from a point-like ideal initial distribution, a transverse dimension of $\sim 30\mu\text{m}$ in $\sim 1\text{ms}$, because of its residual thermal expansion. If the cloud were at room temperature (300°K), after 1ms it would have reached a transverse dimension of 0.5m . Cooling the atoms is therefore necessary to have collimated atomic beams which do not expand too quickly as they propagate along the interferometer.

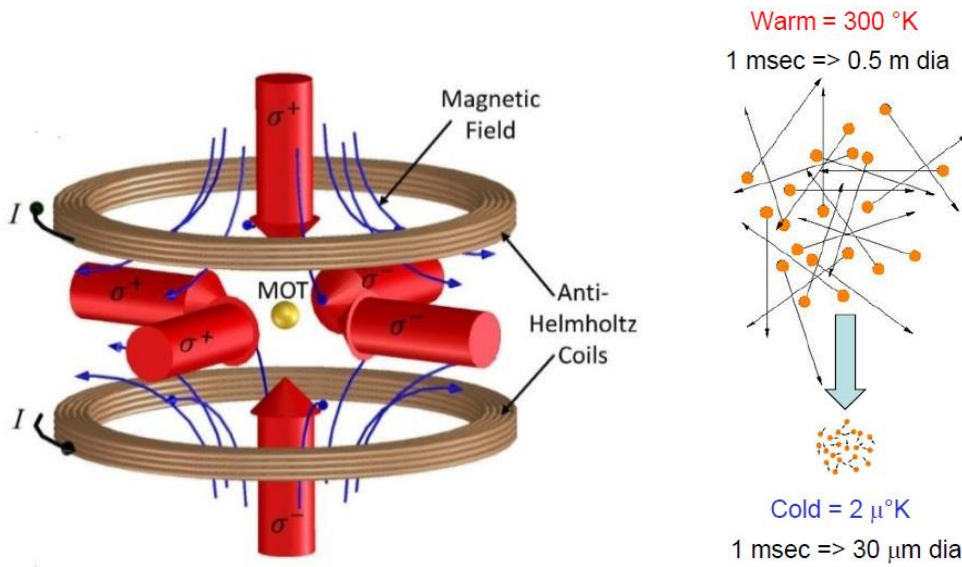


Fig. 3: conceptual scheme of a magneto optical trap (MOT), and typical expansion of a cloud of cold atoms as compared with atoms at room temperature.

In Fig. 4 we show the atomic states of a ^{87}Rb atom involved in the interferometric sequence. The two states of interest are a fundamental state $|f, \mathbf{p}\rangle$ and an excited state $|e, \mathbf{p} + \hbar\mathbf{k}_{\text{eff}}\rangle$. Optical transitions between these two states are induced by exploiting the stimulated Raman effect, which makes use of two counter-propagating laser beams with frequencies ω_1 and ω_2 . The momentum of two atomic states differs by $\hbar\mathbf{k}_{\text{eff}} = \hbar(\mathbf{k}_1 - \mathbf{k}_2) \cong 2\hbar\mathbf{k}_1$, \mathbf{k}_1 and \mathbf{k}_2 being the wave-vectors of the counter-propagating beams.

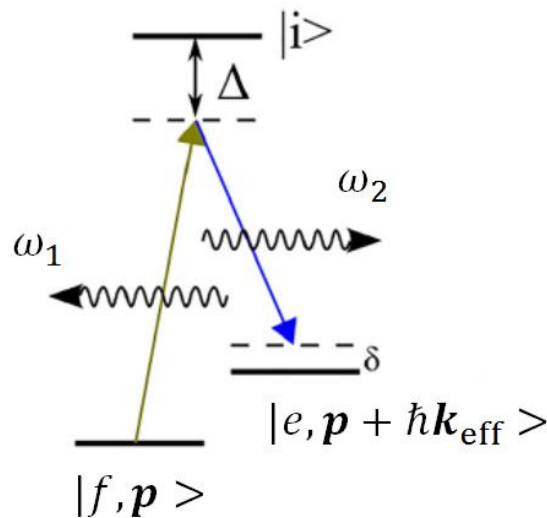


Fig. 4: Atomic states of a ^{87}Rb atom and stimulated Raman transitions induced by counter propagating laser beams.

Fig. 5 show the evolution of the states in which the atom can be as it propagates along the interferometer. The first laser pulse (known in the literature as a $\pi/2$ pulse, and actually formed by a pair of counter-propagating pulses), has properties such as intensity and duration finely calibrated to induce with a 50% probability an atomic transition from the fundamental state $|f, \mathbf{p}\rangle$ in which the atom is before entering the interferometer to the excited state $|e, \mathbf{p} + \hbar \mathbf{k}_{\text{eff}}\rangle$. After such a pulse the atom is in a superposition of the two states, which in rough terms means that it has simultaneously (i) remained in the fundamental state and continued its initial trajectory, following the blue line in Fig. 5, and (ii) transitioned to the excited state, having received a momentum kick of $\hbar \mathbf{k}_{\text{eff}}$ which changed its trajectory to the green line.

After an evolution time T the atom is shone upon by a so-called π pulse, meaning that it is calibrated in such a way to induce an atomic transition with 100% probability. Therefore the excited state (where the atom is with 50% probability) is turned into the fundamental one, and the fundamental state (where the atom is with 50% probability) is turned into the excited one. This is represented in Fig. 5 by changing colour and direction of both the lines which represent the two trajectories the atom is simultaneously in.

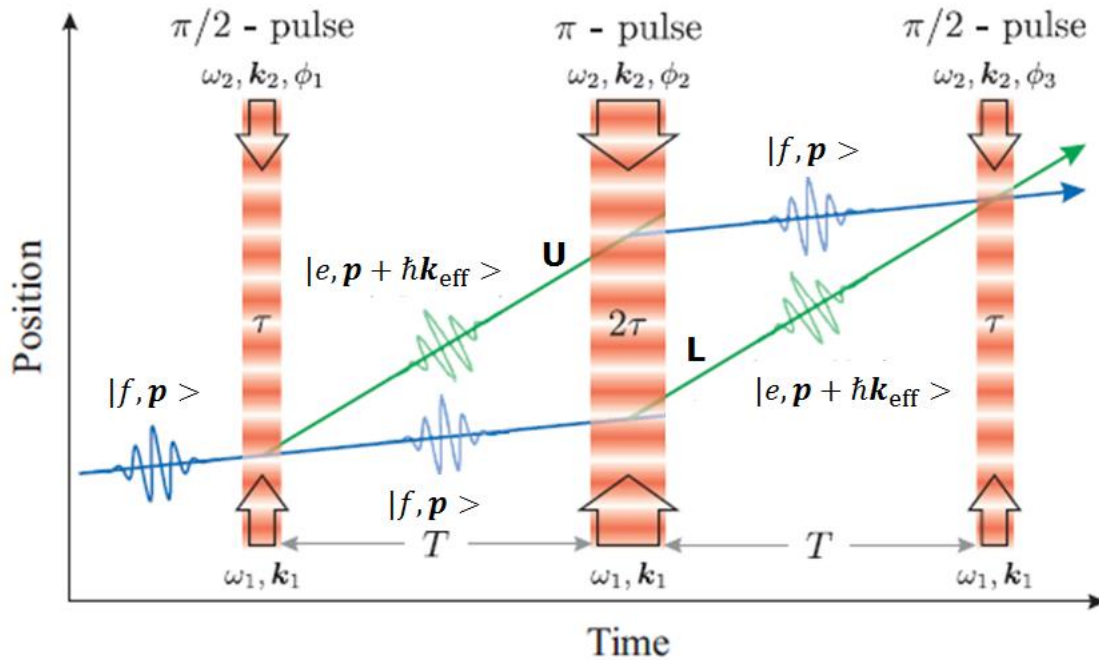


Fig. 5: State of the atom as it evolves inside a three-pulse Mach-Zehnder interferometer. In the figure, τ and 2τ are the duration of the $\pi/2$ and of the π laser pulses respectively, while U and L indicate the upper and the lower paths in the interferometer. Let's give some typical numbers: a cloud with $N \approx 10^6$ atoms propagates inside an interferometer with a longitudinal velocity $v \approx 1 \text{ m/s}$; the interferometric pulses are separated by time intervals $T \approx 10 \cdot 10^{-3} \text{ s}$, and the total length of the interferometer is therefore $v \cdot 2T \approx 2 \text{ cm}$. When excited by a laser pulse, which has a typical duration of 10^{-6} s , an atom acquires an additional transverse velocity component equal to $\Delta v \approx 10^{-2} \text{ m/s}$, so that the spatial separation between the two atomic paths at the centre of the interferometer becomes $\Delta v \cdot T \approx 10^{-4} \text{ m}$.

After another time interval T , a second $\pi/2$ pulse is shone on the atom. Such a pulse turns with 50% probability the fundamental state (where the atom is with 50% probability) into the excited one, and simultaneously it turns with 50% probability the excited state (where the atom is with 50% probability) into the fundamental one. After this pulse the atomic wavefunction is given by the sum of two terms which have equal weight, and are associated respectively with the atom in the fundamental state and in the excited state. These two terms have however different phases: this is due to the fact that each time a laser pulse of the $\pi/2$ - π - $\pi/2$ sequence has interacted with the atom it imprinted on the atomic wavefunction a phase shift equal to its optical phase at the time and position of the interaction, with a sign that depends on the atomic transition it has

induced. The term of the wavefunction describing the atom exiting the interferometer in the fundamental state has therefore acquired a phase φ_U^{light} determined by the green-blue upper trajectory U, while the term describing the atom exiting the interferometer in the excited state has acquired a phase φ_L^{light} determined by the blue-green lower path L. To obtain the atomic probability density we now have to sum these two terms to obtain the total atomic wavefunction, and then square it. The phase difference $\varphi_L^{\text{light}} - \varphi_U^{\text{light}}$ will therefore appear in the function which gives the probability of finding the atom in either of its possible states. In other terms, it could be said that the probability that the atom at the interferometer exit is in its fundamental or in its excited state depends on the difference between the phases it has accumulated while it was simultaneously travelling along the two available paths inside the interferometer.

To show how this effect can be exploited for sensing we will now make the example of a laboratory CAI gravimeter, which measures the acceleration due to a gravitational field g . In this case, the apparatus (and therefore the lasers which generate the optical pulses which imprint their phases on the atomic wavefunction) is fixed to the ground, and the trajectories of the atoms assume a parabolic behaviour under the action of the gravity field, as shown in Fig. 6. The total atomic phase difference between the two paths turns out to be

$$\Delta\Phi = \mathbf{k}_{\text{eff}} \cdot \mathbf{g} T^2 + (\varphi_1 - 2\varphi_2 + \varphi_3)$$

Here the presence of the contribution $\mathbf{k}_{\text{eff}} \cdot \mathbf{g} T^2$ is what gives the interferometer its gravity sensing capability: it is clear that the instrument can be made more sensitive by increasing the time-of-flight T or the momentum \mathbf{k}_{eff} transferred to the atoms by the pairs of laser pulses. With $\varphi_1, \varphi_2,$ and φ_3 are indicated the phases of the three downward Raman pulses with respect to the upward ones. If there are three pairs of independent lasers these three relative phases are under the control of the experimenter: the term in parenthesis can therefore be made to assume the most convenient value, and for simplicity from now on it will be taken as equal to zero.

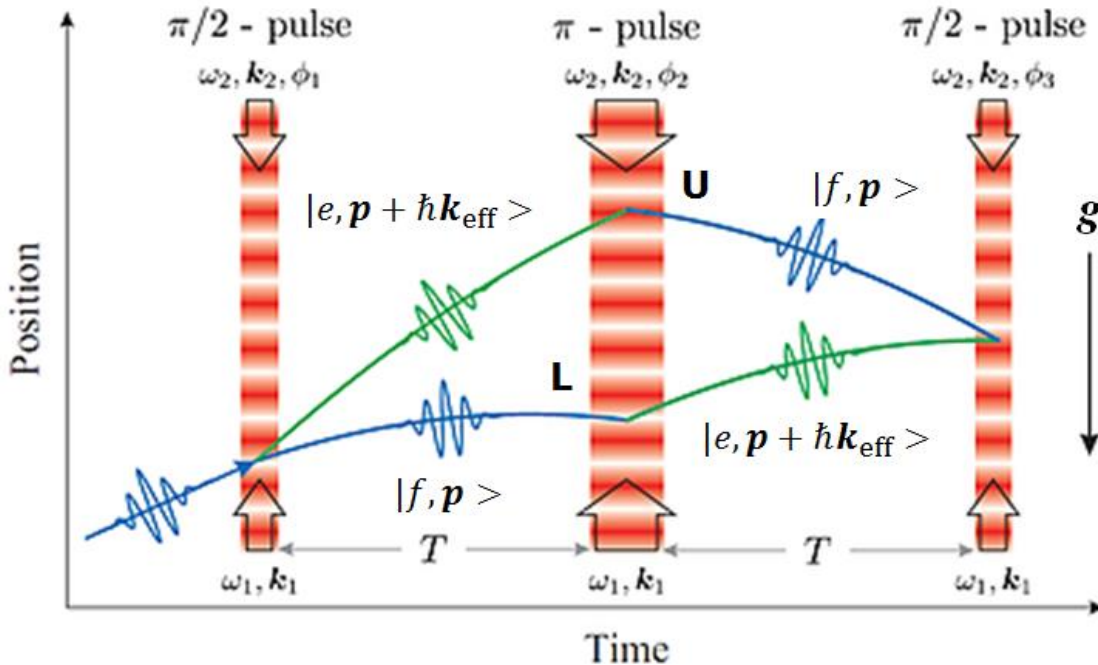


Fig. 6: atomic trajectories in a three pulse interferometer intended to measure the gravitational acceleration.

We are now in the position to better understand why atomic interferometers can be more sensitive than optical ones. Since the velocity of the atoms inside the interferometer is much smaller than the velocity of light ($\sim 1\text{m/s}$ versus 10^8 m/s), the force we are interested in will have a much longer time to interact with the atoms and therefore to

modify the paths they take inside the interferometer. This allows even a very tiny force to induce a measurable contribution to the phase difference $\phi_L^{\text{light}} - \phi_U^{\text{light}}$ which is imprinted onto the atomic wavefunction. The system therefore is not actually exploiting the fact that the atomic wavelength is much shorter than the optical one, since what determines the magnitude of the detected signal is the difference between the *optical* phases which the laser beams imprint on the atomic wavefunction: the phase difference depends on k_{eff} , but not on p . With respect to optical interferometry, the advantage is that even a very small force can contribute to this difference: atoms are much slower than photons, and therefore interact for much longer times with the force to be measured. There is however the other side of the coin: the N atoms which form the cloud going across the interferometer are typically in the $\sim 10^6$ range, and since each of them contributes to the signal independently from the others the final measurement will be affected by a shot noise which scales as $\frac{1}{\sqrt{N}}$. In an optical interferometer, where there are typically 10^{16} photons contributing to the signal, the associated shot noise level will be much smaller. Additionally, it must be considered that for a mix of fundamental reasons and technical constraints the $\pi/2$ and π pulses used in the interferometric sequence to act on the atomic wavefunction are much less efficient than an optical beam splitter.

Coming back to the example of the gravimeter, let us emphasise that any other effect able to modify the trajectories of the atoms and therefore the time and location at which they encounter the interferometric pulses will give rise to a further contribution to $\Delta\Phi$, which would add to the one determined by the gravitational field. Typically, the motion of alkali metal atoms is affected by magnetic fields: on one hand, this means that a CAI-based magnetic field sensor can be envisaged, but on the other it implies that a CAI gravimeter should be accurately shielded from any magnetic field. It is also necessary to damp out any vibrations, since the vertical component of the acceleration associated with such vibrations will end up summed with the gravitational one.

It is also possible to use a CAI to measure the acceleration of the atoms propagating inside it with respect to another moving object. A preliminary step is ensuring that the light emitted by the bottom lasers contains both frequencies ω_1 and ω_2 , and substituting the top Raman lasers in Fig. 6 with a mirror attached to the moving object with respect to which we want to measure the acceleration of the atoms. This arrangement ensures that the phases of the three reflected pulses depend on the mirror position, and this information is imprinted on the atomic wavefunctions. As an outcome, the interferometer will be measuring the atom acceleration with respect to the moving mirror, or conversely the mirror acceleration with respect to the atoms. As we will see in the next section, this approach can be employed to build a hybrid accelerometer. Let's assume that the atoms are motionless in a zero-gravity environment, or moving under the influence of a stationary field, while the mirror is the proof mass of an electrostatic accelerometer subject to several disturbances. The signal coming from the CAI accelerometer can be used to drive a feedback loop that feeds an actuator operating on the proof mass, in such a way to suppress its vibrations and drifts. In this hybrid system the CAI accelerometer is used to obtain a reference signal which is employed to suppress the noise affecting the classical accelerometer.

In addition to measuring the gravitational field, a CAI gravimeter can also be used to investigate more fundamental issues regarding the theory of gravitation. In this case the object of interest is not the magnitude of the gravitational field, but its possible dependence on the mass it is acting on. Such dependence is not contemplated in Newton's theory, but is not ruled out by more general physical models of gravitation. If existent, it is expected to give rise to extremely small effects, and this could be the reason why they have never been detected with the techniques employed until now. CAI has therefore been recruited to this aim. Several experimental efforts are underway, which require the propagation in the interferometer of two atomic species with different masses m_1 and m_2 to detect any possible difference between g_{m_1} and g_{m_2} . In a satellite, the reduced gravitational pull would allow the atoms to remain for longer times inside the interferometer and therefore increase the sensitivity of the CAI measure. In a

microgravity environment, the launched cold atoms move in a uniform velocity: the interrogation time is therefore determined only by the launching velocity, a parameter which can be well controlled by the experimenter. In addition, the absence of gravitational-induced tilts improves the quality of the magnetic confinement.

Let us now imagine a different situation, where no external forces of any kind are acting on the atoms propagating in the interferometer, and thus they are following straight inertial paths; conversely, the instrument (and its lasers in particular) is attached to a moving platform. In these conditions the two paths the atom can take inside the interferometer, and therefore the phase difference $\varphi_L^{\text{light}} - \varphi_U^{\text{light}}$ accumulated by the wavefunction as the atom propagates along them, will be determined by the acceleration and the rotation rate of the platform: this means that the interferometer can assume the role of an inertial sensor such as an accelerometer or a gyroscope. What determines the output of the interferometer is the relative motion of the atoms and of the lasers producing the interferometric sequence: if the atoms are on inertial straight paths, the output will be only determined by the acceleration and the angular velocity of the instrument frame to which the lasers are fastened.

It should be stressed that also in this case great care should be taken to avoid the parasitic effects of magnetic fields and vibrations. However, there is an additional complication: in the presence of a gravitational field, admittedly a quite common situation, a CAI accelerometer will be measuring the sum of the acceleration with which the instrument itself is moving and of the gravitational acceleration which is affecting the motion of the atoms inside it. This follows from the fact that both the motion of the atoms under the action of the gravitational field and the motion of the instrument itself (which in this case constitutes the object of our interest) will contribute to determine the times and positions where the atom meets the laser pulses, and therefore the phase difference $\varphi_L^{\text{light}} - \varphi_U^{\text{light}}$. Indeed, there is no way to distinguish inertial effects from gravitational ones. If the instrument is intended for autonomous navigation, it must therefore be complemented with an independent knowledge of the local gravity field (e.g. a gravitational map), in such a way that the local gravitational component can be eliminated from the measured acceleration.

It can be demonstrated that if the interferometer is designed as an inertial sensor the total phase difference $\Delta\Phi$ is given by the sum of two contributions Φ_a and Φ_Ω determined respectively by acceleration and angular velocity; in explicit terms, it is given by

$$\Delta\Phi = \Phi_a + \Phi_\Omega = \mathbf{k}_{\text{eff}} \cdot \mathbf{a} T^2 + 2\mathbf{k}_{\text{eff}} \cdot (\boldsymbol{\Omega} \times \mathbf{v}) T^2$$

where \mathbf{a} and $\boldsymbol{\Omega}$ are respectively the acceleration and the angular velocity to be measured, and \mathbf{v} is the propagation velocity of the atoms in the interferometer. It is apparent that, for any given laser-induced transition which fixes \mathbf{k}_{eff} , the sensitivity of the instrument increases with the interaction time T , because the same signals \mathbf{a} and/or $\boldsymbol{\Omega}$ will generate a larger phase difference $\Delta\Phi$. It can also be seen that acceleration and angular velocity simultaneously contribute to $\Delta\Phi$, so that some tricks must be used to distinguish among them. A common way to achieve this aim is by using two counter-propagating clouds of atoms (i.e. with opposite values of \mathbf{v}), and then sum and subtract their signals to obtain respectively \mathbf{a} and $\boldsymbol{\Omega}$. This approach entails using two separate MOTs and careful synchronization.

The phase difference determines the transition probability, which is given by

$$P(\Delta\Phi) = \frac{N_e}{N_e + N_f} = P_0 - \frac{C}{2} \cos(\Delta\Phi)$$

where N_e and N_f are the relative atomic populations respectively in the excited and in the fundamental states, P_0 is an offset probability ideally equal to 0.5, and C is the fringe visibility ideally equal to 1. Assuming for P_0 and C their ideal values, we have that a $\Delta\Phi = 0$ leads to $P = 0$ and $N_e = 0$ (no atoms in the excited state), while $\Delta\Phi = \pi$ leads to $P = 1$ and $N_e = 1$ (all atoms in the excited state). Fig. 7 shows how experimental findings

confirm the oscillating pattern predicted by the theory for the transition probability: in practice, from a measurement of the relative population in the two states we deduce the phase difference, and from the phase difference we calculate the signal we are interested in.

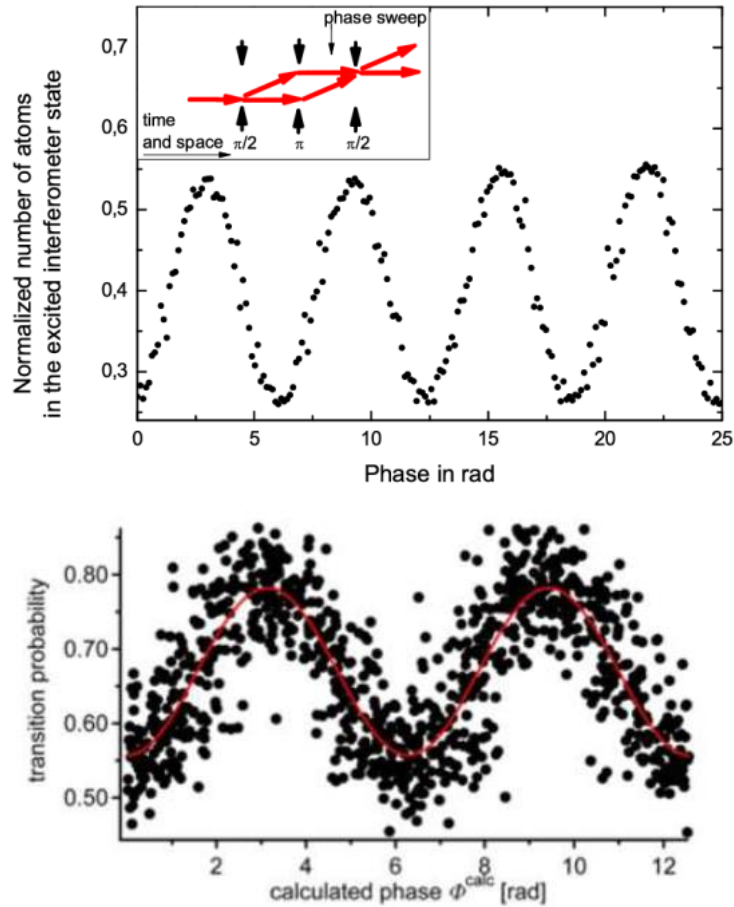


Fig. 7: Experimental points measuring the probability of an atom having transitioned from the fundamental to the excited state.

By considering the results shown in Fig. 7, we can also appreciate the deviations from the ideal behaviour. In particular, the transition probability does not oscillate between 0 and 1, meaning that visibility of the fringes is not unitary and the signal to noise ratio is somewhat degraded. This follows from several technical factors, and among them particularly relevant are those impacting on the efficiency with which the laser pulses induce the desired atomic transitions. One of the factors at play here is that the intensity transverse profile of a laser beam is not uniform and the atomic cloud occupies a finite volume of space: as a consequence, only some of the atoms in the cloud will encounter the exact value of the optical field which is necessary to induce the desired transition, for a given duration of the pulse. This unavoidably implies that (i) the preparation stage does not have a perfect efficiency, meaning that not all of the atoms entering the interferometer are in the desired initial state (ii) some of the atoms will not undergo the expected transitions in the three-pulse interferometer, thus failing to capture in their phases the signal to be measured and (iii) some atoms will not be counted at the detection stage. A possible way to attenuate this problem would be by reducing the physical dimensions of the atomic cloud, but it should be taken into account that any reduction in the number of atoms will increase the shot noise. It must also be considered that the atomic cloud unavoidably grows larger with time, because of the residual thermal agitation of the atoms. This implies an unescapable trade-off between the sensitivity of the instrument and the visibility of the fringes, since the sensitivity of the instrument increase with the time interval spent by the cloud inside the interferometer. A

compromise must also be made between the instrument bandwidth and its sensitivity: a faster instrument requires shorter permanence time $2T$ of the atomic cloud inside the interferometer, but any reduction of T will diminish its sensitivity.

An additional feature to be taken into account follows from the fact that the measurement procedure follows a succession of separate steps: a cloud of atoms is cooled, it is launched and initialized, it passes across the interferometer, and, after it has exited, the relative populations in the two sub-clouds it has been split into are detected, thus allowing plotting one of the points in Fig. 7. The procedure is then repeated with a new cloud of atoms. The useful measurement time is the time spent by the atomic cloud inside the interferometer. All the other steps of the measurement procedure contribute to a so-called "dead time", during which the instrument is only preparing itself for the actual measurement. The dead time constitutes a significant fraction (usually greater than 50%) of the total time necessary to perform a single measurement, and it is mostly due to the time necessary for the MOT to cool the atoms. It has a direct impact on the repetition rate of the instrument, i.e. on the time interval between two successive measurements. Note that if we want to reduce the ballistic expansion of the cloud by reducing the temperature, we would be forced to keep the atom in the MOT for a longer time, thus increasing the instrument dead time. Typically, CAI can make measurements with an overall frequency of some hertz, although several technologies are being tested to improve their repetition rate.

It is also apparent that the output/input relation of a sensor based on CAI is (approximately) linear only for phase intervals much smaller than π , which typically translates in extremely small signals; in addition the periodicity of $P(\Delta\Phi)$ implies that the same output (as measured by the relative populations in the two atomic states) can be attributed to different values of the phase difference, and therefore different values of the signal. This means that CAI-based inertial sensors have very limited dynamical range, and must work in tandem with other conventional sensors whose sensitivity may be lower but whose dynamical range must be wider. Differently put, to successfully track the CAI inertial signals it is necessary that rapid variations in linear acceleration (jerk) and in angular velocity are limited to an amount equivalent to a $\pi/2$ interferometer phase shift over one interferometer cycle. This dictates maximum values for the acceptable jerk and angular acceleration, and exceeding these values requires the use of complementary auxiliary sensors. In this hybrid quantum-classical approach classical sensors are typically used also to measure the disturbances (vibration, magnetic field) which must be filtered out. On the other side, a CAI sensor can act as an absolute reference to provide on-site calibration to classical sensors.

3 Research highlights

The material of this section is divided according to the targeted applications, so we will have a first subsection devoted to inertial navigation which describes CAI-based gyroscopes and accelerometers, and a second subsection dedicated to gravimeters. Although a gravimeter is conceptually identical to an accelerometer, the actual use of the two instruments dictates very different constraints and therefore different implementations. An accelerometer usually needs to be less sensitive than a gravimeter, but has higher requirements in terms of dynamical range, speed, size, power consumption, portability, and ruggedness. In it, acceleration must be measured along three different axis, and a six axis instrument measuring also the three components of the angular velocity is necessary to have a sensor which can be employed in an inertial navigation unit. A gravimeter is a simpler one-axis instrument, since it is intended to measure the vertical (and slow-varying) acceleration associated with the Earth gravity field. It however needs to be extremely sensitive and portable, to allow its employment in gravity surveys. However, by surveying the scientific literature, we noticed that very often the same group of researcher address with their efforts both inertial navigation and gravimetry application, and qualify their devices for both uses. In these cases, gravimeters will be considered accelerometers and therefore included in the first subsection, dedicated to inertial navigation sensors. In the second subsection we will give more space to actual measurement campaigns and field deployments of CAI gravimeters than to the instruments technical details.

3.1 Gyroscopes and accelerometers

In this Section we present some examples of the research activity on the development of gyroscopes and accelerometers based on cold atom interferometry.

For historical reasons, we start by presenting the first experiment which demonstrated an accelerometer based on cold atom interferometry, performed in Stanford in 1991. An atomic fountain with a Mach-Zehnder interferometric scheme based on three stimulated Raman transitions was employed, see Fig. 8. At a 1Hz pulse rate, $\sim 5 \times 10^7$ sodium atoms, confined initially to a ~ 3 mm sphere, were launched on vertical ballistic trajectories. The temperature of the atoms was $\sim 30 \mu\text{K}$, with a rms velocity spread of ~ 30 cm/s. Each pulse of atoms was generated from a three-step sequence which consisted of loading a magneto-optic trap, cooling the trapped atoms, and launching the cooled atoms vertically with a mean propagation velocity of ~ 2.5 m/s. The atoms were trapped and launched in an ultra-high vacuum environment: a liquid nitrogen cooled cryo-shield helped maintain an operating background pressure of $\sim 1 \times 10^{-10}$ torr. A sensitivity to accelerations of $\Delta g/g = 3 \times 10^{-8}$ was demonstrated for $T = 50$ ms drift times, after 2×10^3 seconds of integration time. The authors claimed that by using caesium instead of sodium and by implementing an active vibration isolation system, an absolute sensitivity of $\Delta g/g < 10^{-10}$ can be achieved, exceeding the resolution of falling corner cube gravimeters. They also suggested that advances in diode laser technology and trapping of atoms in vapour cells should make it possible to engineer a portable system for geophysical applications.

In 2006, again in Stanford, a laboratory scale demonstration of a cold atom gyroscope was performed, see Fig. 9. The authors started by noting that high accuracy terrestrial navigation requires a stable rotation output at the $\sim 10^{-3}$ deg/h level for time scales of ~ 84 min, while geodetic applications (e.g. the detection of wobbles in the Earth's rotation rate) require stability at the level of $\sim 10^{-6}$ deg/h over months. Using caesium atoms, they demonstrated an interferometric gyroscope which meets the stability requirements for high accuracy navigation. This was achieved by implementing a technique to precisely reverse the axis of the gyroscope, thus compensating several noise sources. Elaborating on their data and observing the gyroscope rotation output in a nearly static environment, they demonstrate a gyroscope bias stability of $< 70 \times 10^{-6}$ deg/h, a scale factor stability of < 5 ppm, and a short-term noise (as measured by the angle random walk) of $\sim 3 \times 10^{-6}$ deg/h^{1/2}. According to the authors, their bias stability is ~ 300 times better than that

attained by commercial navigation grade ring laser gyroscopes, and their angle random walk is ~ 1000 times better than that associated with ring laser gyroscopes or fibre optic gyroscopes used in navigation-grade inertial navigation systems. According to the authors, a field implementation of their system would enable navigation with a system drift less than 1 km/h.

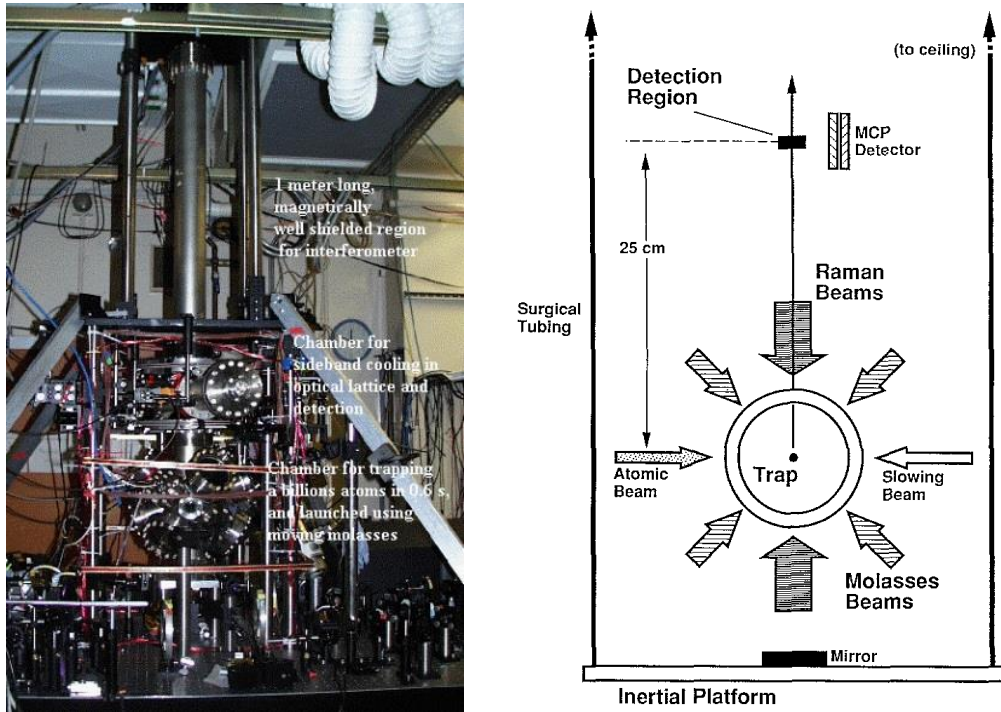


Fig. 8: CAI accelerometer developed at Stanford, 1992⁴.

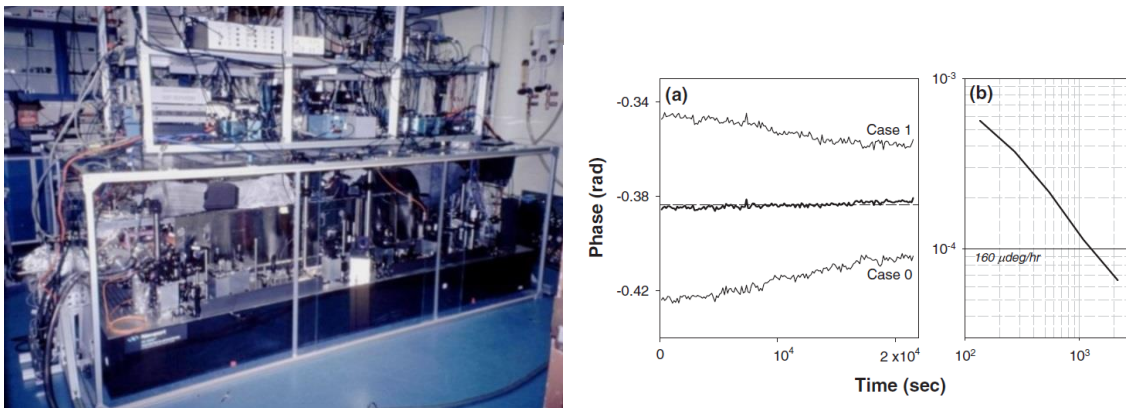


Fig. 9: CAI gyroscope developed at Stanford, 2006⁵.

The Stanford group generated a spin-off company, AOSense, which commercializes cold atom enabling technologies and devices such as atom beams sources, electronics, frequency standards, lasers, fibre frequency combs, optical isolators, transfer cavities, opto-mechanical components, and ion pumps. They have a commercial version of a cold

⁴ "Measurement of the gravitational acceleration of an atom with a light-pulse atom interferometer", M. Kasevich & S. Chu, Applied Physics B, Vol. 54, 321–332, 1992; <https://link.springer.com/article/10.1007/BF00325375>

⁵ "Long-Term Stability of an Area-Reversible Atom-Interferometer Sagnac Gyroscope", D. S. Durfee et al., Phys. Rev. Lett. 97, 240801, 2006; <https://journals.aps.org/prl/abstract/10.1103/PhysRevLett.97.240801> <https://arxiv.org/pdf/quant-ph/0510215.pdf>

atom gravimeter to be used for geophysics applications, and are working on compact versions of inertial sensors. According to their website, "AOSense is a leading developer and manufacturer of innovative atom optic devices for precision navigation, gravity measurement, and timekeeping. Our capabilities include gyroscopes, accelerometers, inertial measurement units (IMUs), gravimeters, gravity gradiometers, and atomic frequency standards. Atom optic devices use frequency-stable lasers to manipulate atoms freely falling in a vacuum cell, resulting in unparalleled accuracy and stability that greatly surpasses the performance of conventional designs. AOSense was formed in 2004 by Brenton Young and Mark Kasevich to spin-off innovative research developed at Stanford University, joined by Jim Spilker as Chairman. In 2006, AOSense was awarded its first prime contract from DARPA to design, build, and test a gravity gradiometer and single axis accelerometer/gyroscope. Since then, AOSense has successfully designed and built state-of-the-art cold atom technology for numerous government sponsored programs funded by DARPA, Air Force, Army, Navy, NASA, NSF, DTRA, and the intelligence community".

A compact system which allows measuring all the six components of acceleration and angular velocity is needed to build an IMU. A six-axis inertial sensor has been developed in Paris by SYRTE by using two MOT to generate counter-propagating atomic clouds, and laser pulses coming from different directions with respect to the atomic trajectory plane. Such a layout allows measuring both $[a_x, a_y, a_z]$ and $[\Omega_x, \Omega_y, \Omega_z]$, as shown in Fig. 10. Caesium atoms are cooled down to $3 \mu^\circ\text{K}$, and atomic clouds are generated every 0.56 s^{-1} and launched into the interferometer at 2.4 m s^{-1} . The interrogation sequence is achieved with a single pair of Raman beams covering the entire interrogation zone. The atomic velocity and the Raman beam size (30 mm diameter) set the maximum interrogation time to 60 to 80 ms. Acceleration and rotation sensitivity of $4.7 \times 10^{-6} \text{ m} \cdot \text{s}^{-2}$ and $2.2 \times 10^{-6} \text{ rad} \cdot \text{s}^{-1}$ have been reached for 1 s averaging time, and of $6.4 \times 10^{-7} \text{ m} \cdot \text{s}^{-2}$ and $1.4 \times 10^{-7} \text{ rad} \cdot \text{s}^{-1}$ for 10 min averaging time. For long integration times, the Allan standard deviation approaches a white noise behaviour, thus offering projection-noise-limited performance with a sensitivity to acceleration and rotations of $5.5 \times 10^{-7} \text{ m} \cdot \text{s}^{-2} \text{ Hz}^{-1/2}$ and $2.4 \times 10^{-7} \text{ rad} \cdot \text{s}^{-1} \text{ Hz}^{-1/2}$ respectively.

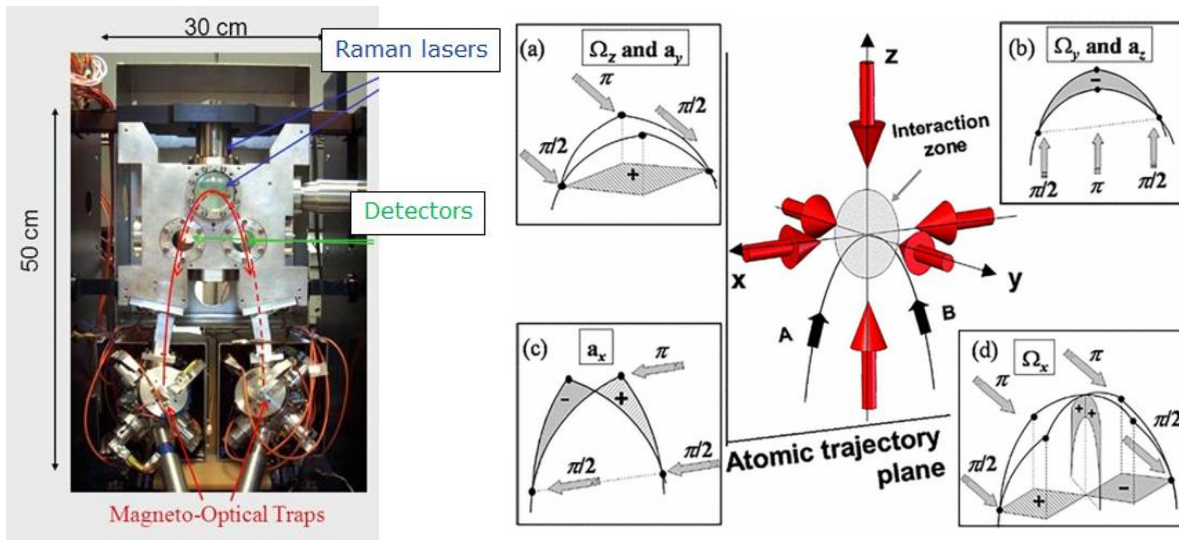


Fig. 10: Six-axis inertial sensors developed in Syrte, 2006⁶.

⁶ "Six-Axis Inertial Sensor Using Cold-Atom Interferometry", B. Canuel et al., Phys. Rev. Lett. 97, 010402, 2006
<https://journals.aps.org/prl/abstract/10.1103/PhysRevLett.97.010402>
<https://arxiv.org/pdf/physics/0604061.pdf>

Because of its high sensitivity, running a CAI usually requires low-vibration and high-thermal stability environments that can only be found in dedicated ground or underground platforms. The first operation of a matter-wave inertial sensor in an aircraft was reported by a team including Onera, see Fig. 11. Their matter-wave interferometer uses ^{87}Rb atoms and operates aboard the Novespace A300 – 0g aircraft, which carries out parabolic flights during which 22s ballistic trajectories at 0g are followed by 2min of standard gravity flight at 1g. The interferometer measures the local acceleration of the aircraft with respect to an inertial frame of reference attached to the free-falling interrogated atoms. Telecom-based laser sources are used to guarantee high-frequency stability and power in a compact and integrated setup. Starting from a ^{87}Rb vapour, a cloud of about 3×10^7 atoms is cooled down to $10 \mu\text{K}$; the atoms in the appropriate magnetic-insensitive state and in the right velocity range are then selected, so that $\sim 10^6$ of them enter the accelerometer. The Raman laser beams are aligned along the plane wings direction (Y axis) and are retroreflected by a mirror attached to the aircraft structure and following its motion. The CAI therefore provides a measurement of the relative mean acceleration of the mirror along the Y axis during the interferometer duration. In the aircraft, the acceleration along Y fluctuates over time, and is at least three orders of magnitude greater than the typical signal variations recorded by laboratory-based matter-wave inertial sensors. To quantify the information contained in the atomic measurements, mechanical accelerometers (MAs) fixed on the retroreflecting mirror are employed, and the correlation between the MAs and the CAI is analysed. The instrument consists therefore of a hybrid sensor that is able to measure large accelerations due to the mechanical devices, and able to reach a high resolution because of the atom accelerometer. The CAI signal is limited by the imperfections of the atomic beam splitters and mirror due to the temperature of the cloud and to the gaussian intensity profile of the Raman beams, whereas the main contribution to noise comes from the detection process. On the classical side, better scale factor calibration of the MAs and the damping of high frequency vibration ($>10\text{Hz}$) are required to improve the setup.

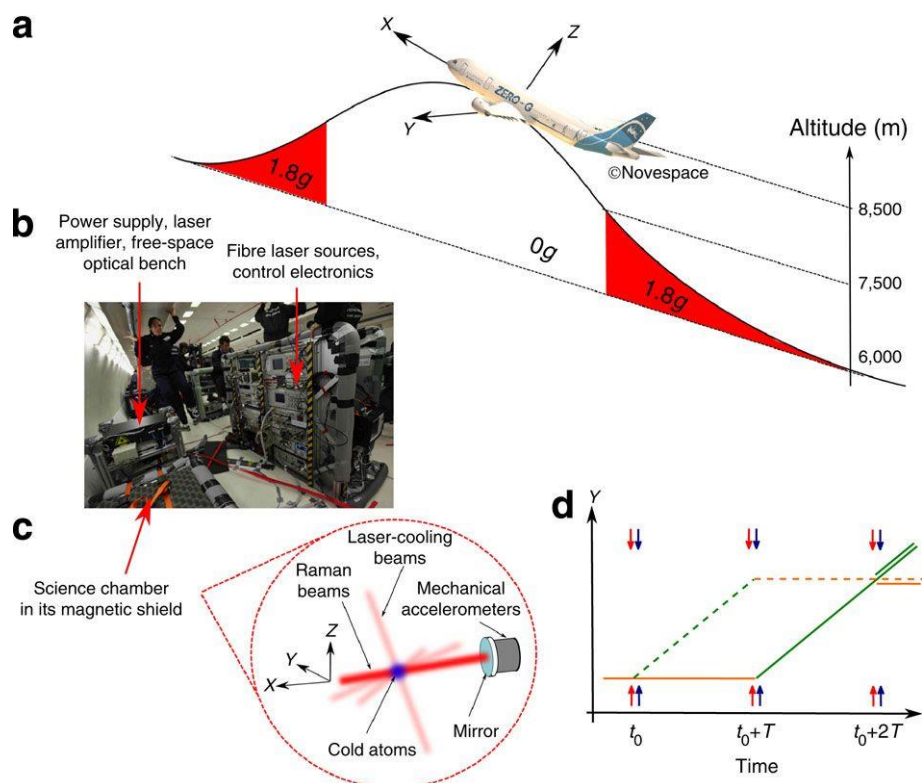


Fig. 11: Operation of a CAI accelerometer on-board a 0g aircraft, 2011⁷.

⁷ "Detecting inertial effects with airborne matter-wave interferometry", R. Geiger et al., Nature Communications Vol. 2, N. 474, 2011; <https://www.nature.com/articles/ncomms1479>

At $1g$, the sensitivity level of the combined sensor reaches a level of $1.6 \times 10^{-3} \text{ m s}^{-2} \text{ Hz}^{-1/2}$, and is able to measure inertial effects more than 300 times weaker than the typical acceleration fluctuations of the aircraft. At $0g$, a vibration noise rejection scheme is investigated: it makes use of a four-pulse scheme to build a two-loop interferometer equivalent to two successive one-loop interferometers head to tail. The resulting signal is given by the coherent subtraction of two spatially and temporally separated inertial measurements, and is therefore expected to be less sensitive to the low-frequency inertial effects. An estimated sensitivity of $2 \times 10^{-4} \text{ m s}^{-2} \text{ Hz}^{-1/2}$ has been obtained, which paves the way for an extension of the method to airborne and spaceborne tests of the universality of free fall with matter waves.

A compact inertial sensor was developed by the Rasel group in Hannover, see Fig. 12. An atomic cloud at $10 \mu\text{K}$ is launched in the interferometer with a forward velocity of 4.4 m/s , so that for a total interferometer time $2T=2 \text{ ms}$ the interferometer effective length is about 9 mm . The atomic ensemble has a radius of 2.2 mm in the middle of the interaction zone, while the Raman beams have a diameter of 30 mm . With a total interrogation time of $2T=4 \text{ ms}$ a sensitivity of $2 \times 10^{-3} \text{ m/s}^2/\text{Hz}^{1/2}$ for accelerations and $2 \times 10^{-4} \text{ rad/s}/\text{Hz}^{1/2}$ for rotations is demonstrated. Several technical improvements are suggested which would allow improving these results, and reaching a rotation rates sensitivity of $\sim 10^{-9} \text{ rad/s}$ for one second of measurement. Using an extended interferometer scheme with three independent atom-light interaction zones would further enhance the performances, achieving sensitivities better than $10^{-8} \text{ rad/s}/\text{Hz}^{1/2}$.

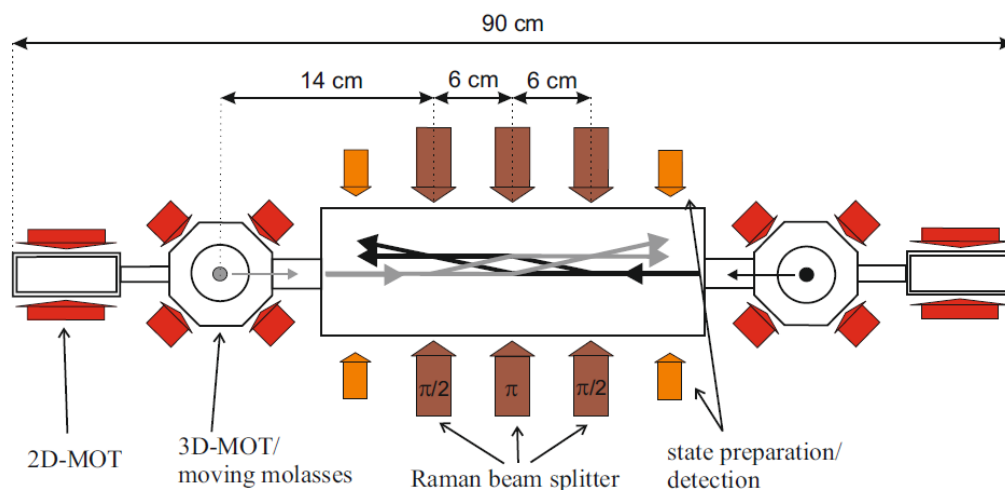


Fig. 12: Hannover compact CAI gyroscope⁸.

A collaboration involving Sandia targeted a higher measurement frequency by exploiting cold atom recapturing, see Fig. 13: the idea is that recycling as many cold atoms as possible reduces the dead time associated with the cooling process. In their device, two ^{87}Rb atom ensembles are cooled to $35 \mu\text{K}$ in 1.5 ms inside two MOTs located 3.6 cm apart, and are launched toward one another at a velocity of 2.5 m/s . During their ballistic trajectory, they are interrogated with a stimulated Raman sequence, detected, and then recaptured with an estimated efficiency of 85% in the opposing trap zone. The time between two successive Raman pulses is 4.1 ms , and the π pulse duration is $1.6 \mu\text{s}$. A dual-axis measurement sequence, involving a single vector component for the acceleration and the angular velocity, can be realized in 16.6 ms . Thus is realized a combined accelerometer and gyroscope having a frequency measurement of 60 Hz , with sensitivities to acceleration and rotations of $8.8 \times 10^{-6} \text{ m} \cdot \text{s}^{-2} \text{ Hz}^{-1/2}$ and $1.1 \times 10^{-6} \text{ rad s}^{-1} \text{ Hz}^{-1/2}$ respectively.

⁸ "A compact dual atom interferometer gyroscope based on laser-cooled rubidium", T. Müller et al., The European Physical Journal D, Vol. 53, 273–281, 2009; <https://link.springer.com/article/10.1140/epjd/e2009-00139-0>

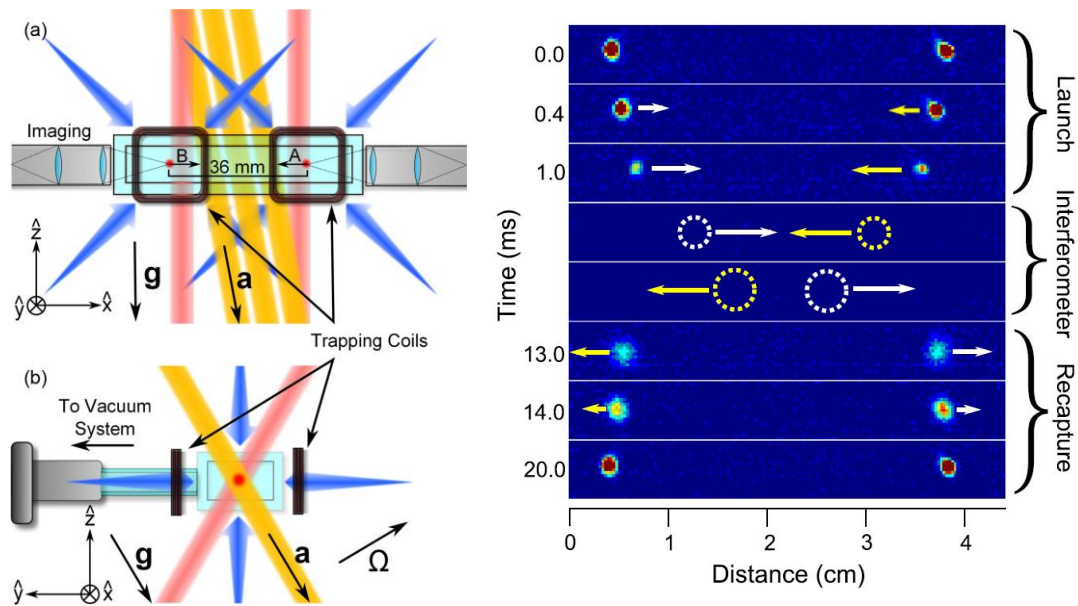


Fig. 13: Cold atom recapturing by Sandia, 2014⁹.

A sensor hybridization scheme was proposed by Syrte in 2014, see Fig. 14. The author started by observing that the sequential operation of CAI sensors leads to dead times between consecutive measurements, which causes an intrinsic low frequency sampling ($\sim 1\text{Hz}$) of the vibration noise and an aliasing effect of the high-frequency noise components. The use of active or passive isolation platforms to overcome the problem leads to bulky set-ups ill-suited for operation in noisy or mobile environment. Increasing the cycling frequency can attenuate the problem, but at the price of a sensitivity reduction. An alternative method exploits post-correlations between simultaneous measurements from classical and atom accelerometers. This resolves the ambiguity in the fringe number which is typical of cold-atom interferometers: their sensitivity is indeed so high that typical urban vibrations induce atomic phase shifts greater than π , which scatters the measurement points away from mid-fringe over several interference fringes. Exploiting ex-post correlation between classical and quantum signal leads however to a sub-optimal sensitivity, as measurement performed at the top and bottom of the fringes have low sensitivity to phase fluctuations.

In their work the authors exploit this correlation, but they now pre-compensate the atomic phase fluctuations induced by vibrations in a real-time way, acting on the phase difference of the Raman lasers before the wavepackets are recombined. In addition to suppressing vibration noise, this enhances the instrument sensitivity by keeping it operating at mid fringe. Furthermore, they take the full advantage of these correlations to correct for the drift of the mechanical accelerometer. They claim a short-term sensitivity of $6.5 \times 10^{-7} \text{ ms}^{-2}$ at one second measurement time, improving up to 300 s to reach a level of $3 \times 10^{-8} \text{ ms}^{-2}$. The hybrid sensor combines the advantages of both sensors, providing a continuous and broadband (DC to 430 Hz) signal which benefits from the long term stability and accuracy of the atomic sensor. These features make it appealing for geoscience (seismology and gravimetry), and are of major relevance in inertial navigation. Indeed, since the high frequency variation of the acceleration is the signal of interest for the calculation of the trajectory of the vehicle, any loss of information induced by dead times constitutes a major limitation. Using the hybrid accelerometer for calibration would allow reaching an error of less than 1 m after 4 h of navigation.

⁹ "Dual-Axis High-Data-Rate Atom Interferometer via Cold Ensemble Exchange", Akash V. Rakholia et al., Physical Review Applied, Vol. 2, N. 054012, 2014; <https://arxiv.org/pdf/1407.3847.pdf>
<https://journals.aps.org/prapplied/abstract/10.1103/PhysRevApplied.2.054012>

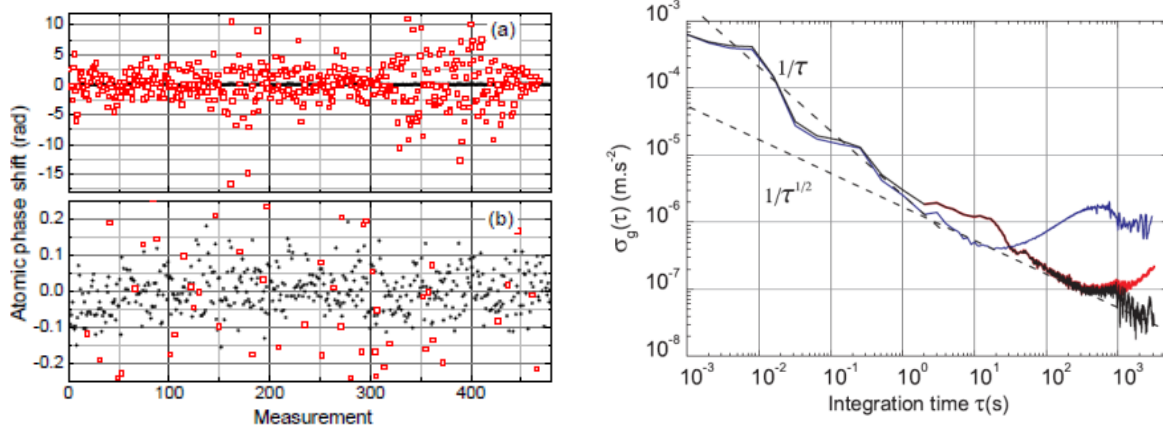


Fig. 14: Quantum-classical hybridization, Syrte 2014. Left: Open red squares represent the atomic phase shifts estimated from the classical accelerometer, while full black points give the atomic phase shifts measurements when compensated for vibrations in real time. Right: Allan standard deviation of acceleration signals: conventional accelerometer alone (blue line), hybrid accelerometer without (red line) and with (black line) correction from Earth's tides¹⁰.

An additional way to improve the performance of CAI has been introduced by Rasel's group, and exploits the use of composite light pulses to create beam splitters and mirrors. The resulting symmetrized composite-pulse interferometer (SCI) differs from the MZI scheme since it does not require a preparation step prior to the interferometer sequence and the beam splitter and the mirror are composed of a rapid succession of Raman pulses separated by a minimal dark time, see Fig. 15. The immunity of the SCI to noninertial perturbations stems from the fact that most of the time - namely, during the time T of free evolution - the matter waves are in the same electronic state while propagating along the two branches. Therefore, the fluctuations of both the phase of the laser which drives the transition between these states and the external forces which, in general, act differently on the two internal states, only affect the interferometer signal during the comparably small time intervals τ (single pulse duration) and t_s (dark time) and are therefore strongly reduced as compared to the MZI. The suppression of these noise effects is best quantified in terms of the temporal sensitivity function $g(t)$. In Fig. 15 is shown the space-time diagram ($x; t$) and the corresponding sensitivity function $g(t)$ for (a) a conventional Mach-Zehnder interferometer (MZI) with single Raman pulses (red wavy lines) as atom-optical elements and (b) the symmetrized composite-pulse interferometer (SCI) featuring multiple Raman pulses (multiple red wavy lines) for each atom-optical beam splitter and mirror. Note that τ as well as t_s within a composite pulse are not drawn to scale. The Raman interactions lead to a change of both the electronic state (ground and excited state denoted by solid and dashed lines, respectively) and the kinetic momentum of the wave packet, depending on the direction of the effective photon momentum k (indicated by black arrows). The contrast of the MZI signal depends crucially on the state preparation. A pure sample of excited-state atoms can be achieved by optical pumping after molasses cooling. We recall that molasses cooling makes use of three pairs of circularly polarized laser beams to cool neutral atoms to temperatures lower than a magneto-optical trap (say tens of $\mu^\circ\text{K}$ instead of hundreds of $\mu^\circ\text{K}$); however, unlike a MOT, no trapping is provided. As shown in the figure, a specific velocity class of this sample can be selected with the help of a Raman pulse transferring them into the ground state, while the rest of the excited atoms are removed by a resonant blow-away pulse (yellow wavy lines). In contrast, in the SCI the blow-away pulse is not performed until the first two beam-splitter pulses. As indicated by $g(t)$, which expresses the sensitivity to Raman laser phase noise and magnetic field fluctuations, the

¹⁰ "Hybridizing matter-wave and classical accelerometers", J. Lautier et al., Appl. Phys. Lett. Vol. 105, No. 144102, 2014, <https://aip.scitation.org/doi/pdf/10.1063/1.4897358>
<https://arxiv.org/pdf/1410.0050.pdf>

SCI is insensitive to these noise sources during the free evolution time T , while the MZI is most sensitive during the same period.

The authors therefore demonstrate an interferometer with a high immunity to technical noise, with a rotation rate sensitivity of $120 \times 10^{-9} \text{ rad s}^{-1} \text{ Hz}^{-1/2}$, with which they determined the Earth's rotation rate with a relative uncertainty of 1.2%. They claim that their atom interferometer surpasses current cold atom gyroscopes in sensitivity, and that the composite light pulses method can be employed in other applications or in tests of the foundations of physics. In particular, the immunity to noise can be exploited in very long baseline atom interferometers, where large magnetic shields and low-noise lasers for coherent manipulation of the atoms are required.

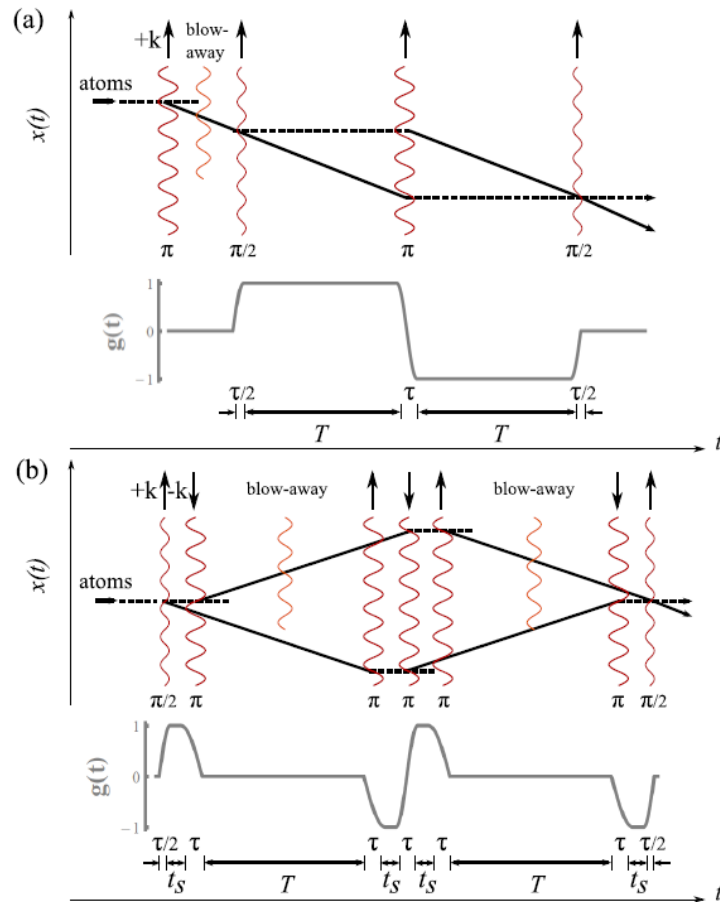


Fig. 15: The symmetrized composite-pulse interferometer (SCI) propose by Rasel's group¹¹.

In fundamental physics, CAIs may provide new answers to the question of whether the free-fall acceleration of a particle is universal, that is, independent of its internal composition and quantum properties. Although the so-called universality of free fall (UFF) principle has been tested experimentally to a few parts in 10^{13} , various extensions to the current theoretical physics framework predict its violation. It is thus important to develop more sensitive experimental techniques to test these theoretical models. Advances towards the use of cold atom accelerometers in this framework were made in 2016 by using a 0g plane, see Fig. 16. Tests of the UFF generally involve measuring the relative acceleration between two different test masses in free fall with the same gravitational

¹¹ "Composite-Light-Pulse Technique for High-Precision Atom Interferometry", P. Berg et al., Phys. Rev. Lett. Vol. 114, No. 063002, 2015; <https://journals.aps.org/prl/abstract/10.1103/PhysRevLett.114.063002>

field, and are characterized by the Eötvös parameter. Presently, the most precise measurement of this parameter using atom interferometry has been carried out with the two isotopes of rubidium at the level of a few 10^{-8} , which is still five orders of magnitude less precise than the best tests with classical bodies. This has motivated increasing the sensitivity of matter-wave interferometers (which scales as the square of the free-fall time) by circumventing the limits set by the gravitational free fall on Earth, either by building a large-scale vertical apparatus or by letting the entire set-up fall in an evacuated tower. This is also one of the main goals for space-borne experiments, where the satellite can be viewed as an ideal 'Einstein elevator'. The experiment, where two matter-wave sensors composed of rubidium (^{87}Rb) and potassium (^{39}K) operate simultaneously in the weightless environment produced by parabolic flight (Fig. 53), represents an atom-interferometric test of the UFF in microgravity. Despite the significant challenges given by large vibration levels and variations in acceleration and rotation rates onboard the aircraft present, the authors demonstrate the capability of their correlated quantum system by measuring the Eötvös parameter with systematic-limited uncertainties of 1.1×10^{-3} and 3.0×10^{-4} during standard- and microgravity, respectively. These results indicate that the developed system can be applied to inertial navigation, and can be extended to the determination of the trajectory of a satellite for future space missions.

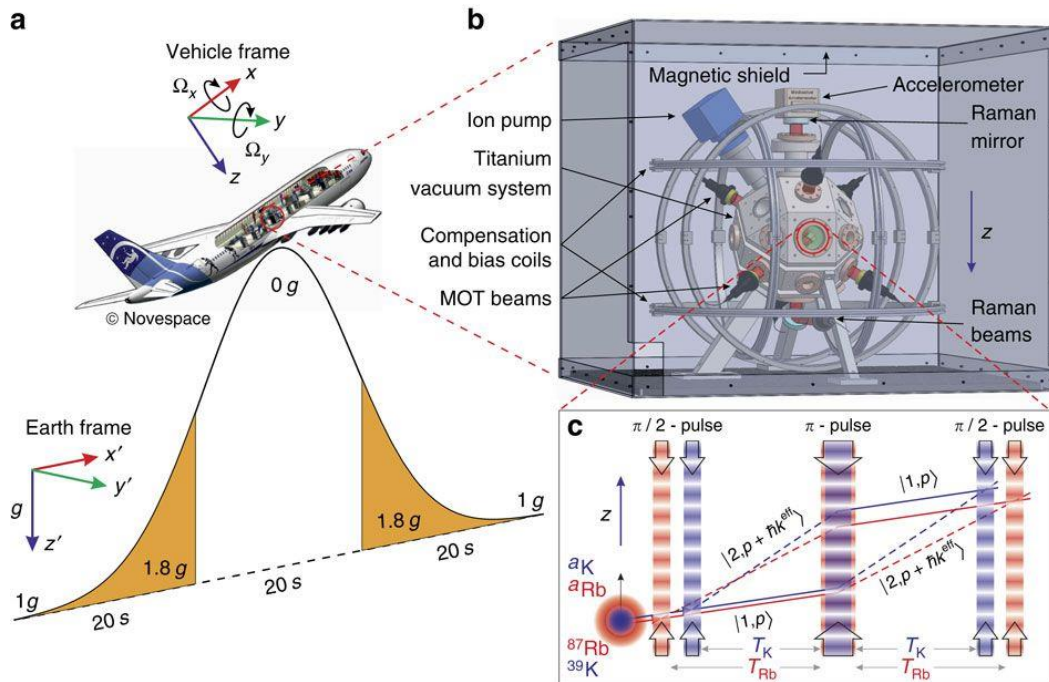


Fig. 16: Overview of the 2016 experiment using a dual-species accelerometer on-board a 0-g plane. a) Basic trajectory during parabolic flight (b) On-board science chamber, with laser-cooled samples of ^{87}Rb and ^{39}K and Raman beams aligned along the z axis of the aircraft (c) Schematic of the simultaneous dual-species interferometers¹².

A different way to achieve both high sampling rates and high inertial sensitivities is by resorting to atom juggling schemes, where several atomic clouds are simultaneously travelling inside the device. Syrte in 2018 demonstrated a cold-atom gyroscope where an atomic cloud is cooled while three previously launched clouds are interrogated in the interferometer in an interleaved way, featuring an interrogation time of 801 ms at a sampling rate of 3.75 Hz, see Fig. 17. The atoms are loaded in the MOT during 55ms, and $2 \cdot 10^5$ atoms are detected at the end of the interferometer. Thanks to the use of auxiliary sensors, a servo loop is implemented to guarantee a real-time compensation of linear acceleration noise and to allow operating the interferometer at mid-fringe, i.e. in

¹² "Dual matter-wave inertial sensors in weightlessness", Brynle Barrett et al., Nature Communications, Vol. 7 N. 13786, 2016; <https://www.nature.com/articles/ncomms13786>

its linear range, which increases its sensitivity. The interleaved operation also averages rotation noise and allows reducing the impact of residual linear acceleration noise. Because the sampling frequency (3.75 Hz) is higher than the frequencies at which the acceleration noise mostly contributes (around 0.5 Hz), correlations appear between successive measurements, yielding a scaling of the sensitivity that approaches t^{-1} rather than $t^{-1/2}$. From the Allan deviation of the gyroscope stability the improvement of the sensitivity as t^{-1} for integration times up to ≈ 7 s is clear; the stability then gradually enters the $t^{-1/2}$ regime characteristic of uncorrelated white noise, corresponding to a sensitivity of $3 \cdot 10^{-8} \text{ rad s}^{-1} \text{ Hz}^{-1/2}$, while the bias stability is $\sim 3 \cdot 10^{-10} \text{ rad s}^{-1}$.

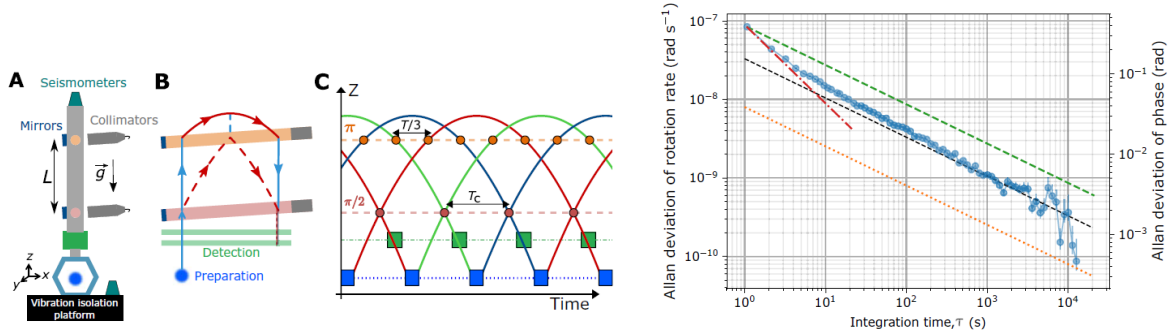


Fig. 17: Interleaving atomic clouds to increase sensor bandwidth and sensitivity¹³.

Advances towards the development of a compact multi-axis inertial sensor are being carried on by the iXAtom laboratory, in collaboration between iXBlue and LP2N. This group is also working on accelerometer hybridization, see Fig. 18. Indeed, they note that currently the long-term bias stability of navigation-grade accelerometers is of the order of $10 \mu\text{g}$ which, in the absence of aiding sensors such as satellite navigation systems, leads to horizontal position oscillations of 60m at the characteristic Schuler period of 84.4 minutes. However, cold-atom-based sensors generally possess a small bandwidth, and suffer from low repetition rates and dead times during which no inertial measurements can be made, which hinders their use for inertial navigation systems. In comparison, mechanical accelerometers exhibit broad bandwidths compatible with navigation applications, but are afflicted by long-term bias and scale factor drifts.

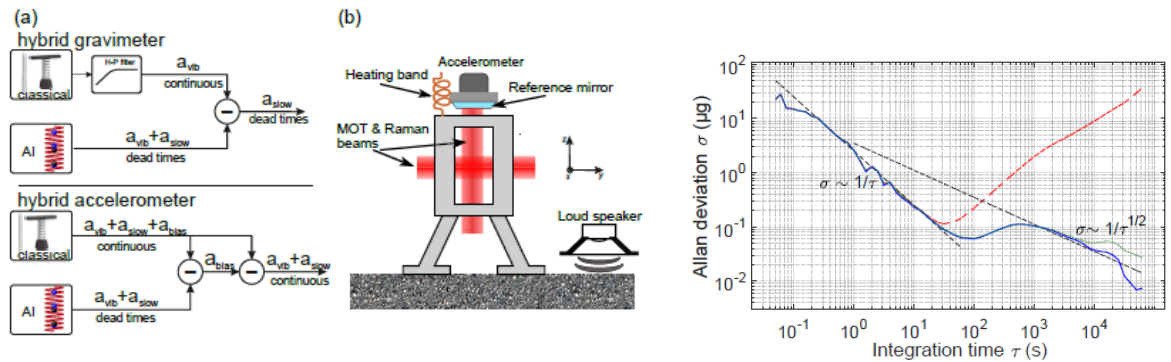


Fig. 18: iXBlue and LP2N collaboration on hybrid sensors, 2018¹⁴.

¹³ "Interleaved atom interferometry for high-sensitivity inertial measurements", D. Savoie et al., Science Advances, Vol. 4, N. 12, 2018; <https://advances.sciencemag.org/content/4/12/eaau7948> <https://arxiv.org/pdf/1808.10801.pdf>

¹⁴ "Navigation-compatible hybrid quantum accelerometer using a Kalman filter", P. Cheiney et al., Physical Review Applied Vol. 10, N. 034030, 2018; <https://arxiv.org/pdf/1805.06198.pdf> <https://journals.aps.org/prapplied/abstract/10.1103/PhysRevApplied.10.034030>; See also "Development of a compact cold atom sensor for inertial navigation", SPIE Photonics Europe (Brussels), 2016, published in Quantum Optics, Vol. 9900 (2016) <https://doi.org/10.1117/12.2228351>

The authors therefore use correlations between an atomic interferometer and a classical accelerometer to track the bias of the latter, and use a non-linear Kalman filter to optimally track all of the interference fringe parameters to make the estimation of the accelerometer bias robust against variations of experimental parameters. They simulate a mobile environment in the laboratory by adding simultaneously vibration noise, temperature variations and laser intensity fluctuations. Even under these conditions, they were able to track the fast (400Hz) classical accelerometer bias to less than 1 μg . In a typical laboratory environment, the hybrid accelerometer reaches a precision of 10 ng (10^{-7} ms^{-2} , 10 μGal) after 11 hours of integration. We recall that a Galileo (symbol Gal, abbreviation gal) is a unit of acceleration used extensively in the science of gravimetry: $1\text{Gal}=1\text{cm/s}^2$; 1micro Galileo or μGal : $1\mu\text{Gal} = 10^{-8}\text{m/s}^2 = 10\text{nm/s}^2 \cong 10^{-9}\text{g}$, where $g \approx 9.81\text{m/s}^2$.

In most light-pulse atom-interferometer techniques, the thermal expansion of the cold-atom cloud is an unavoidable unwanted effect which reduces the fringe contrast. Conversely, point-source atom interferometry (PSI) utilizes the thermal expansion of the cold-atom cloud to map the velocity dependent phase shifts onto an imaging plane. In PSI, the Raman pulse sequence is applied to an isotropically expanding cloud of atoms in which each atom interferes only with itself. The thermal velocity spread of the expanding cloud creates many Mach-Zehnder interferometers spanning all directions in a single operation. Each atom generates an interferometer phase that depends on its initial velocity. The strong position-velocity correlation for atoms in the expanded cloud preserves the phase shifts that are detected as an image, with spatial fringes arising from rotations imprinted on the population, see Fig. 19. From the fringe pattern, the acceleration in the propagation direction of the Raman-laser beams and the projection of the rotation vector onto the plane perpendicular to that direction can be measured simultaneously. The sensitivities for the magnitude and direction of the rotation-vector measurement are $0.033^\circ/\text{s}$ and 0.27° with an averaging time of 1 s, while the fractional acceleration sensitivity is $\delta g/g = 1.6 \times 10^{-5} \text{ Hz}^{-1/2}$. These performances are currently limited by the Raman-laser phase noise and the vibration noise.

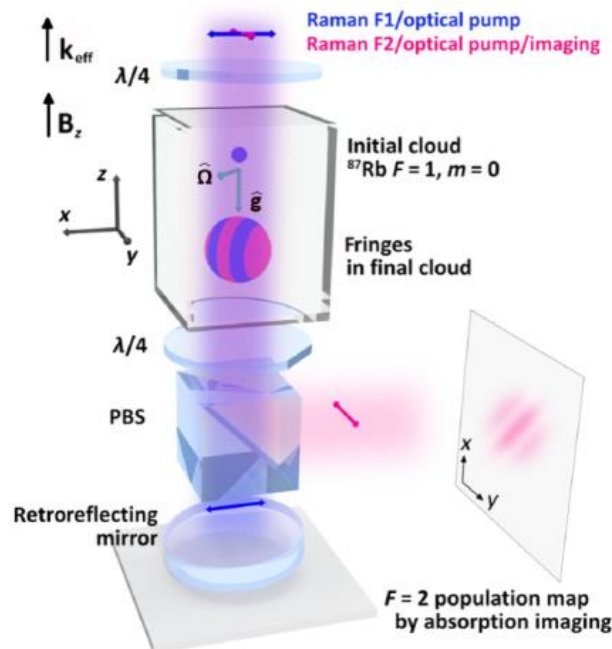


Fig. 19: Point-source atom interferometry¹⁵.

¹⁵ "Single-Source Multi-axis Cold-Atom Interferometer in a Centimeter-Scale Cell", Yun-Jih Chen et al., Physical Review Applied, Vo. 12, N. 014019, 2019; <https://arxiv.org/abs/1812.00106>
<https://journals.aps.org/prapplied/abstract/10.1103/PhysRevApplied.12.014019>

3.2 Gravimeters and gravity gradiometers

In this subsection we will present some highlights on research regarding portable gravimeters and gravity gradiometers based on cold atom interferometry to be used for in-field applications. Although spring-based gravimeters and falling corner cube gravimeters are popular transportable instruments, atomic ones are developing rapidly. Atomic and classical gravimeters have been compared in the laboratory. Spring-based gravimeters can measure gravity variations with a sensitivity of tens of $\mu\text{Gal}/\text{Hz}^{1/2}$, but their accuracy depends on the compensation of spring drifts and reference to gravity stations with known absolute gravity. Falling corner cube gravimeters can measure the absolute value of the local gravity, but their mechanical dropping and lifting system may not be suitable for continuous long-term operations. CAI gravimeters typically reach sensitivities of 5 to $100\mu\text{Gal}/\text{Hz}^{1/2}$ in the laboratory, and portable atomic gravimeters which can continuously measure absolute gravity with sensitivity and accuracy comparable to classical gravimeters are now becoming available, also commercially. Such instrument could be employed for several applications, such as assessing geophysical phenomena (seasonal aquifer fluctuations, ice mass changes, subsidence in low-lying areas, volcanic activities), monitoring resources (ground water, geothermal reservoirs), and detect underground features (cavities, mineral prospecting). In addition, gravity reference maps to aid inertial marine navigation require the use of on-board gravimeters with at least milliGal accuracy. We will therefore focus on the technological status of portable gravimeters and provide examples of how they have been used in the field. At the end of this subsection we will describe some large scale devices, to provide the reader an idea of the ultimate performances which have been obtained and can be of interest for scientific applications.

A group from University of California (Berkeley), the U.S. Geological Survey, and Lawrence Berkeley National Laboratory, recently demonstrated laboratory and field operation of a mobile atomic gravimeter with a sensitivity of $37\mu\text{Gal}/\text{Hz}^{1/2}$ and a half an hour stability of $\sim 2\mu\text{Gal}$, see Fig. 20. Their atomic gravimeter measures absolute gravity in the laboratory with an uncertainty of $20\mu\text{Gal}$, confirmed by a spring-based relative gravimeter referencing to a site with known absolute gravity. In-field gravity measurements have been obtained with a resolution of around $0.5\text{mGal}/\text{Hz}^{1/2}$, depending on environmental noise. A gravity survey in the Berkeley Hills along a route of $\sim 7.6\text{ km}$ and an elevation change of $\sim 400\text{ m}$ has been performed. At each static measurement location, it took about 15 min to set up the gravimeter and a few minutes to measure gravity with an uncertainty of around 0.04mGal .



Fig. 20: Berkley gravimeter and gravity survey path¹⁶.

¹⁶ "Gravity surveys using a mobile atom interferometer", Xuejian Wu et al., Science Advances Vol. 5, N. 9, 2019, <https://advances.sciencemag.org/content/5/9/eaax0800>

The gravimeter geometry features a magneto-optical trap (MOT) inside a pyramid mirror with a through-hole. Cesium clouds are loaded in the pyramidal MOT and then freely fall into the region of fluorescence detection, at a temperature of $2\mu\text{K}$. A magnetic shield and a solenoid around the vacuum chamber create a uniform magnetic bias field. The retroreflector consists of a flat mirror and a quarter-wave plate. The vibration isolation stage includes a passive vibration isolation table, a seismometer, voice coils, and an active feedback loop. A typical Mach-Zehnder interferometer geometry is adopted, with three laser pulses which split, redirect, and combine a matter wave. The atomic gravimeter was installed in a cart of 1m by 0.8m by 1.7m. It weighs around 100 kg, mostly because of the lithium battery power supply, vibration isolation stage, and cart. The cart has two columns, one for the electronic system and the other for the vacuum system. The laser unit consists of two optical breadboards of 60 cm by 46 cm placed at the top level of the cart. The total power consumption is about 250 W. For field operation, the gravimeter was powered by a 1450-W-hour lithium power station, and a fuel-led generator was used as a backup power supply.

A group with researchers coming from several French institutions and a commercial startup has developed a portable absolute quantum gravimeter named MuQuans AQG-A01, see Fig. 21. They claim that it can be operated by a non-specialist staff in real world conditions, both for continuous observatory measurements and gravity mapping, with a setup time at a measurement location of ~ 20 min and a warm-up time of ~ 1 h.

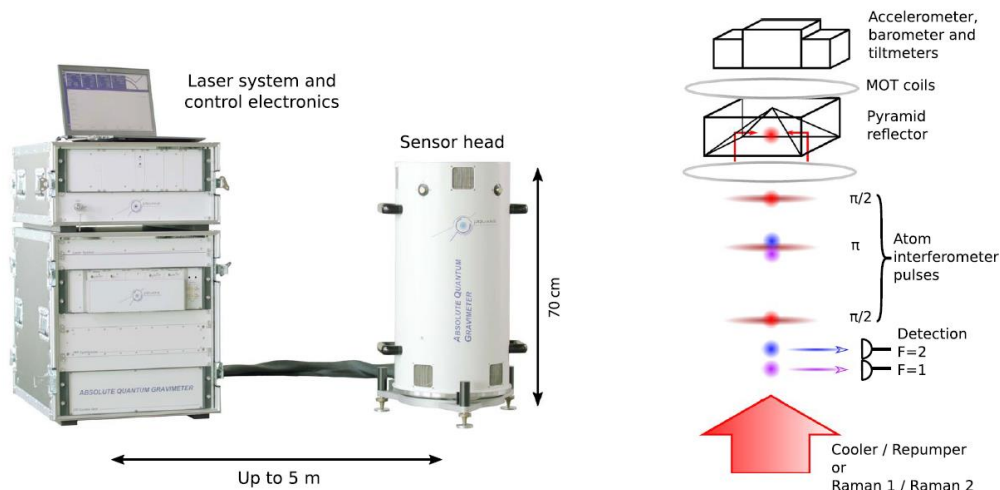


Fig. 21: MuQuans absolute CAI gravimeter¹⁷.

The sensor head (30Kg) is based on a hollow pyramid reflector and a compact telecom based laser system. Approximately 10^7 atoms are loaded in a magneto-optical trap inside the pyramid and cooled down to $2\mu\text{K}$, before being launched in the interferometer where they are interrogated for $T = 60\text{ms}$. The instrument measures gravity at a 2 Hz repetition rate with a sensitivity of $500 \text{ nm/s}^2/\text{Hz}^{1/2}$ (corresponding to $50\mu\text{Gal}/\text{Hz}^{1/2}$) and a long term stability below 10 nm/s^2 (corresponding to $1\mu\text{Gal}$). The single-shot sensitivity floor of the instrument $\delta g/g$ is 3×10^{-8} , a figure deteriorated by laser phase noise or vibrations; the performance is improved by averaging over time to reach a long-term relative stability $\delta g/g = 10^{-9}$. The operation of the gravimeter relies on a classical accelerometer that is utilized to filter out seismic noise, allowing the instrument to be installed directly on the ground without any vibration damping. The MuQuans AQG-A01 gravimeter participated to several comparison campaigns with other instruments and performed gravity measurements at the Laboratoire Souterrain à Bas Bruit, in Rustrel (France) in the frame of the MIGA project, demonstrating a sensitivity of 10^{-8} g at 1 second without the vibration insulating platform.

¹⁷ "Gravity measurements below 10^{-9} g with a transportable absolute quantum gravimeter", V. Ménot et al., Scientific Reports, Vol. 8, 12300, 2018, <https://www.nature.com/articles/s41598-018-30608-1.pdf>

Researchers from a German-Swedish team report on absolute gravity measurements with a mobile quantum gravimeter based on atom interferometry, conducted in Germany and Sweden over periods of several days, see Fig. 22. Superconducting gravimeters (SCG) and falling corner-cube-gravimeters (FCCG) were employed for comparisons. The mobile CAI gravimeter demonstrated an accuracy of 39nm/s^2 and a long-term stability of 0.5nm/s^2 , with a short-term noise of $96\text{nm/s}^2/\text{Hz}^{1/2}$. According to the authors, such performances in a transportable instrument enable new applications in geodesy and other related fields, such as continuous absolute gravity monitoring with a single instrument under rough environmental conditions.

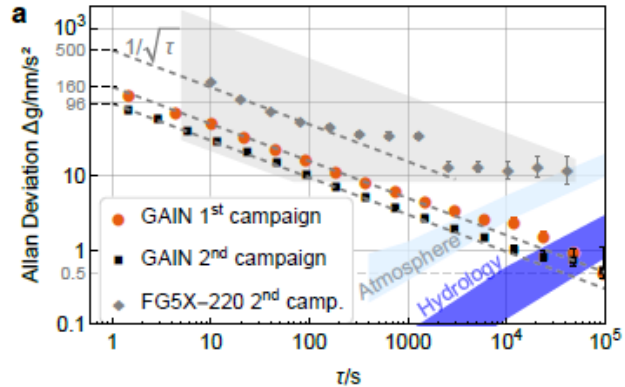
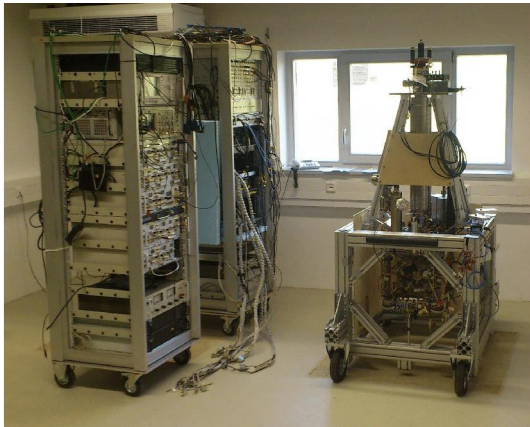


Fig. 22: The GAIN gravimeter and its Allan deviation during two gravity measurement campaigns in which it was compared with the commercial free-fall corner cube gravimeter FG5. The relative stability of the atom gravimeter is 0.5nm/s^2 , or $5 \times 10^{-11}\text{g}$, for a time-scale of 10^5 s (~ 1 day)¹⁸.

A cloud of ^{87}Rb atoms at $2\mu\text{K}$ is launched upwards (fountain configuration) with a vertical velocity of 4m/s . The Raman pulse sequence has a time interval $T=0.26\text{s}$ between pulses, and the measurement cycle time is 1.5 s. The inertial reference is provided by a retro-reflection mirror which is decoupled from environmental vibrations by an active vibration isolation system. Residual micro-seismic noise at $0.1\text{--}0.3$ Hz is detected by a feedback loop error signal, which is fed into a post-correction algorithm to further reduce the interferometer phase noise. The entire system consists of 3 modular units with sizes of $1 \times 1 \times 2\text{m}^3$.

A general advantage of atomic gravimeters compared to FCCGs is that they can compensate micro-seismic excitation, and they do not give rise to floor vibrations as the test-masses involved in the measurement are negligible. These properties enable low noise operation not only on dedicated concrete pillars but also on regular flooring, extending the range of possible measurement sites. In combination with continuous, drift-free, and absolute measurement, CAI gravimeters enable applications such as monitoring of tidal, hydrological or geophysical gravity signals with amplitudes in the 1 to 10nm/s^2 range on long time-scales, where spring-based instruments are limited by non-linear drifts. Albeit the GAIN gravimeter cannot yet reach the ultimate low short-term noise level provided by SCG, the values demonstrated in the paper are comparable to those of state-of-the-art spring-based relative gravimeters without their long-term drifts. It is expected that the noise level of mobile atomic gravimeters will be improved through further optimization of vibration isolators, hybrid sensor strategies or advanced techniques such as interleaved fountain operation.

The Huazhong University of Science and Technology (China) has well-known competences on cold atom interferometry for gravity measurement, as bears testimony a

¹⁸ "Mobile quantum gravity sensor with unprecedented stability", C. Freier et al., 8th Symposium on Frequency Standards and Metrology, Journal of Physics: Conference Series 723, 012050, 2016 <https://iopscience.iop.org/article/10.1088/1742-6596/723/1/012050>

review paper published in 2015, see Fig. 23. As a background, the authors note that commercially available spring-based relative gravimeters are compact and suitable for field work, with a noise level of $\sim 0.1\mu\text{Gal}$. The superconducting relative gradiometer, which has reached a precision of $0.01\mu\text{Gal}$ after one minute integration, can't be used in the field. The absolute corner-cube free-fall commercial FG-5 gravimeter has reached a sensitivity of $10\mu\text{Gal}/\text{Hz}^{1/2}$ and an accuracy of $2\text{--}5\mu\text{Gal}$. Also atomic-fountain CAI gravimeters have reached μGal level sensitivity. Trapped atom gravimeter exploiting optical lattices have also been built, but their sensitivity is typically lower than that of the free fall gravimeter: they are however of scientific interest for the allow measuring short range forces.

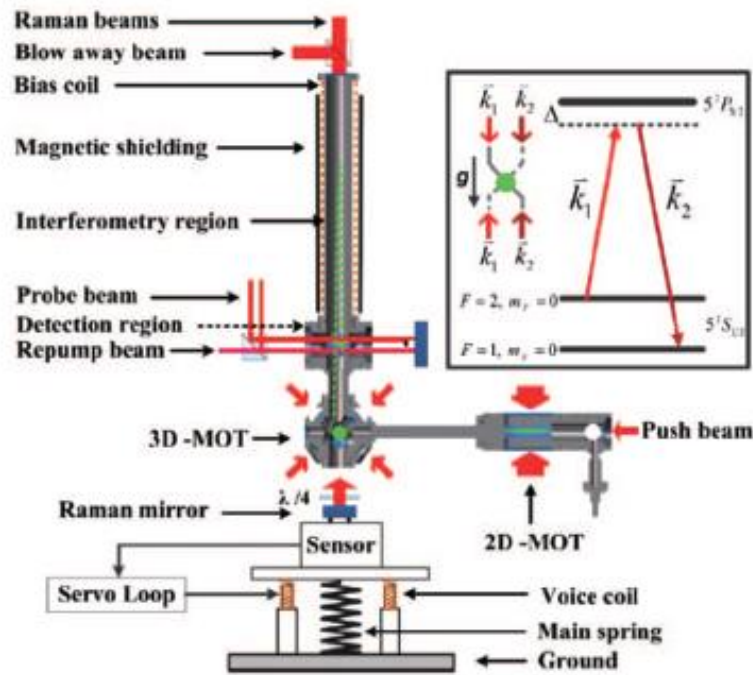


Fig. 23: Gravimeter at Huazhong University of Science and Technology¹⁹.

In the gravimeter developed at HUST, atoms are vertically launched with an initial velocity of $\sim 3.8\text{m/s}$, corresponding to a flight apex of about 0.75m relative to the MOT center. About 5×10^7 atoms with a temperature of about $300\text{n}^\circ\text{K}$ undergo the interferometric sequence, and the time taken for a single measurement is 1s . A Raman mirror is placed under the MOT chamber, to realize the counter-propagating configuration by retroreflecting the Raman beams. To realize the vertical vibration isolator a three-axis commercial seismometer is employed instead of a single-axis accelerometer, which allows obtaining the horizontal vibration data, which can be used to analyze the vibration coupling between the vertical and horizontal directions.

The device guarantees a resolution of about $0.8\mu\text{Gal}$ in 40s , and better than $0.5\mu\text{Gal}$ in 100s . The short-term sensitivity in this same time frame is $4.2\mu\text{Gal}/\text{Hz}^{1/2}$, as given by the Allan deviation. The same group is working also on a gravity gradiometer, demonstrating a short-term sensitivity of $670\text{E}/\text{Hz}^{1/2}$ with a 0.25Hz sampling rate²⁰. The symbol E stands for Eötvös, which is the unit of gradient of gravitational acceleration: $1\text{E} = 10^{-9}\text{s}^{-2}$.

¹⁹ "Micro-Gal level gravity measurements with cold atom interferometry", Zhou Min-Kang et al., Chinese Physics B, Vol. 24, N. 5, 2015; <https://iopscience.iop.org/article/10.1088/1674-1056/24/5/050401>

²⁰ "Operating an atom-interferometry-based gravity gradiometer by the dual-fringe-locking method", Xiao-Chun Duan et al., Phys. Rev. A 90, 023617, 2014; <https://journals.aps.org/pr/abstract/10.1103/PhysRevA.90.023617>

A compact and portable laser system for high-sensitivity fountain-type cold atom gravimeters has been developed by the Wuhan Institute of Physics and Mathematics, see Fig. 24. Using homemade miniaturized optics a laser source, frequency control, power amplification, and beam splitting were integrated into one module of 45×45×16 cm, which provides all the functions (e.g. 2DMOT, moving molasses, and normalized detection) required by high-sensitivity atom gravimeters. The system is used in a fountain-type 85Rb atom gravimeter (fountain height of 36 cm, corresponding to a fountain time of ~540ms), which performs a single measurement in 1.54s, including a loading time of ~1s. Three Raman pulses are utilized to manipulate the atoms, and the atoms' free evolution time between the pulses is $T=200\text{ms}$. A typical interference fringe contains 40 measurements, and it takes nearly 126s to give a value of gravity. They performed a continuous measurement of gravity for 35 h, obtaining results which are consistent with the theoretical curve of the Earth's tides. The measurement sensitivity has been calculated to be $28\mu\text{Gal}/\text{Hz}^{1/2}$, and is limited mainly by the residual vibration noise. After an averaging time of 4000s, the measurement uncertainty is $\sim 0.7\mu\text{Gal}$. Together with the gravimeter, the laser system has been transported by trucks and operated in different environments. In each transport, the laser system always restores to good operating status without internal realignment. In October–November 2017 the units were transported by truck from Wuhan to Beijing ($\sim 1200\text{km}$) to attend the International Comparison of Absolute Gravimeters (ICAG 2017).

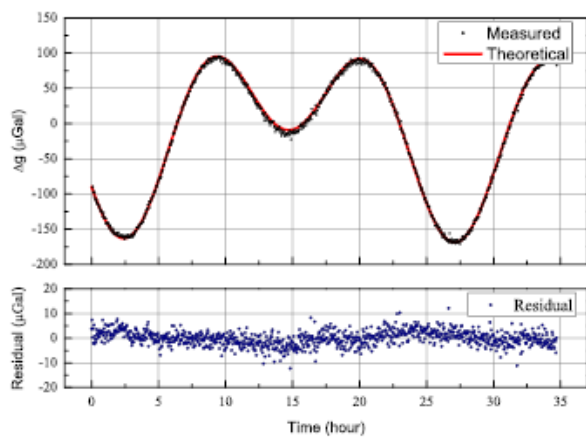


Fig. 24: Compact laser system for a fountain-type CAI gravimeter²¹.

A work demonstrating airborne cold atom gravimetry was funded by the French defence agency (DGA), ESA, ONERA and DTU Space, see Fig. 25. Since only relative sensors are today available for airborne gravimetry, the development of a CAI absolute gravimeter which can be used for airborne gravimetric surveys would enable several applications and eliminate operational constraints and measurement errors. The paper reports the first use of such an instrument. Preliminary tests on a motion simulator lead to gravity measurements noise of $\sim 0.3\text{mGal}$. An airborne campaign was realized across Iceland in April 2017, giving gravity measurements with an estimated error between 1.7 and 3.9mGal. The airborne measurements have also been compared to ground gravity data showing differences with standard deviations and mean value also in the mGal range. The atom sensor is combined with a classical Honeywell Qflex force balanced accelerometer, to give a first rough estimation of the acceleration in order to determine which value of acceleration corresponds to the signal of the atom sensor and to measure the acceleration during the measurement dead times of the atom sensor which occur during the cold atoms preparation and during the detection. On the other hand, the atom accelerometer allows estimating the bias of the classical accelerometer and thus

²¹ "Compact portable laser system for mobile cold atom gravimeters", Xiaowei Zhang et al., Applied Optics, Vol. 57, Issue 22, 2018; <https://www.osapublishing.org/ao/abstract.cfm?uri=ao-57-22-6545>

improving its precision. According to the authors, the gyro-stabilized platform which supports the system and the hybridization algorithm between the classical and the atom accelerometer can be further optimized for airborne environment, allowing their CAI absolute gravimeter to reach the state of the art with sub-mGal precision on airborne survey. They also suggest that their results show the maturity of cold atom technology for on-board application and support the development of atom interferometry sensor for measuring the Earth gravity field from space.

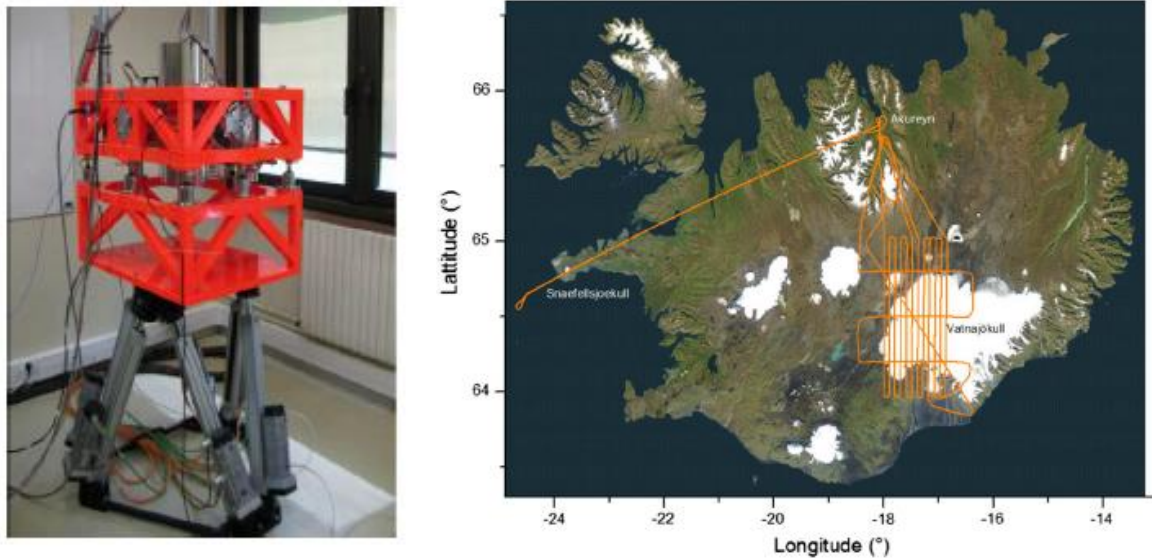


Fig. 25: GIRAPE gravimeter for Iceland airborne gravity survey²².

Measuring Earth's gravity field from satellites provides a spatial resolution limited to ~ 100 km; over sea areas, resolutions of 16 km can be reached by using radar satellite altimetry. Higher spatial resolutions (which are essential in geodesy, geophysics, mineral and hydrocarbon exploration, and navigation) can only be obtained with airborne or shipborne measurements. Today, only relative sensors are available for on-board gravimetry: this constitutes a major drawback because of the calibration and drift estimation procedures which lead to important operational constraints. Atom interferometry is a promising technology to obtain on-board absolute gravimeter. But, despite the high performances obtained in static condition, no precise measurements were reported in dynamic. A paper (see Fig. 26) authored by a group including Onera researchers presents absolute gravity measurements from a ship with a CAI sensor, demonstrating a precision of $\sim 10^{-5} \text{ ms}^{-2}$ (1mGal), in line with a commercial spring gravimeter.

The atom gravimeter has been tested on a ship used by the French hydrographic and oceanographic office to realize gravity surveys for marine needs with a spring gravimeter KSS32M. The surveys with the atom gravimeter were done in North Atlantic Ocean to the west of French Brittany. The atom is used in combination with a force balanced accelerometer (Q- Flex from Honeywell). The classical accelerometer is used to give a first rough estimation of the acceleration in order to determine which value of acceleration corresponds to the signal of the atom sensor. The classical accelerometer is also used to measure the acceleration during the measurement dead times of the atom sensor which occur during the cold atoms preparation and during the detection. The filling of the measurement dead times is very important because vibrations at the repetition rate of the atoms sensors and its multiple can cause an important degradation of sensitivity due to aliasing effect.

²² "Absolute airborne gravimetry with a cold atom sensor", Yannick Bidet et al., Journal of Geodesy Vol. 94, N. 20, 2020; <https://link.springer.com/article/10.1007/s00190-020-01350-2>
<https://arxiv.org/pdf/1910.06666.pdf>

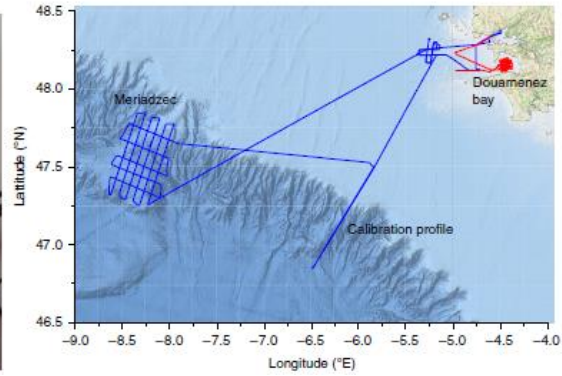
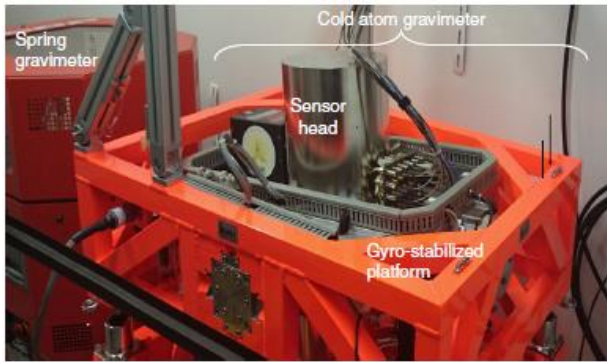


Table 1 Gravimeters results and comparison				
			Atom gravimeter	Spring gravimeter
Calibration profile (9 kn)	Forward-Backward	Mean	0.4	1.8
		Std.	0.5	0.9
	Forward-Reference	Mean	-0.2	1.2
		Std.	0.5	1.1
Backward-Reference	Mean	-0.6	-0.5	
	Std.	0.3	0.6	
Meriadzec (9 kn)	Crossing points difference	Error	0.9	1.0
Douarnenez straight profiles (9 kn)	Forward-Backward	Mean	0.1	0.1
		Std.	0.2	0.8
Douarnenez circular profiles (8 kn)	Crossing points difference with regular profile	Error	0.4	1.0
		Mean	-0.2	1.0
Douarnenez circular profiles (11 kn)	Crossing point difference with regular profile	Std.	0.5	1.0
		Mean	0.3	2.8
		Std.	0.6	2.9

All the values are in mGal. The gravity measurements were filtered with a spatial resolution of 0.8 km for the calibration profile and Douarnenez and 3 km for Meriadzec. The sea state was 6 for the calibration profile and Meriadzec and 4 for Douarnenez

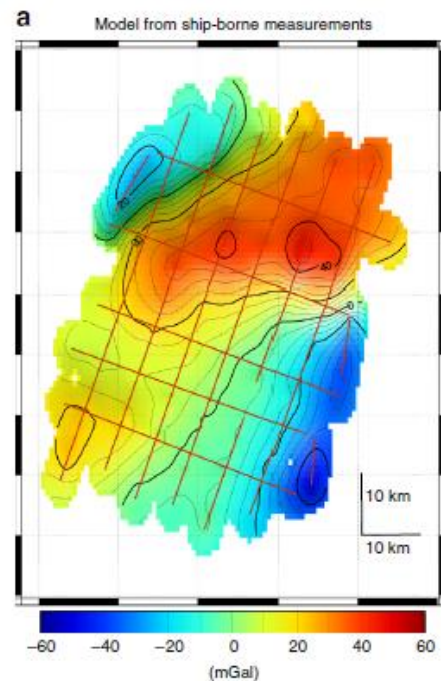


Fig. 26: Results of the October 2015 and January 2016 shipborne gravity survey²³.

The CAI group at Birmingham University is working on portable gravimeters and in particular developing a gravity gradiometer to be used for civil engineering applications^{24,25}. The rationale is that in-field gravity measurements are affected by various kinds of environmental disturbances. This causes a need to integrate over long times, making gravity sensing much slower than competing techniques; but it also inhibits the use of more precise sensors, since in order to resolve smaller signals they would require even longer averaging times. Since the primary coupling of a number of disturbances (e.g. tides, waves) is through vertical acceleration, their effect can be strongly suppressed through adoption of gravity gradient sensing: this relies on simultaneously detecting gravity on two sensors identical in terms of drift and calibration and separated by a vertical baseline. In contrast with two mass-on-spring based

²³ "Absolute marine gravimetry with matter-wave interferometry", Y. Bidel et al., Nature Communications Vol. 9, 627, 2018; <https://www.nature.com/articles/s41467-018-03040-2>

²⁴ "A portable magneto-optical trap with prospects for atom interferometry in civil engineering" A. Hinton et al., Philos Trans A Math Phys Eng Sci. 375(2099), 2017; <https://royalsocietypublishing.org/doi/10.1098/rsta.2016.0238>

²⁵ <http://assessingtheunderworld.org/wp-content/uploads/2016/05/12086-GG-Tops-brochure-Final.pdf>

systems, atom interferometry offers the ability to directly couple two zero-drift sensors, by passing one measurement beam through both atom clouds and referencing a single mirror. This results in both atom clouds measuring the same environmental noise, and these being strongly suppressed through subtraction, see Fig. 27. The Birmingham gravity gradiometer is built around a pyramidal MOT design, in which a single input beam is split by prisms to achieve three counter-propagating beam pairs. This drastically reduces both the size of the optical delivery system and vacuum chamber, by reducing the number of inputs, and the complexity of the laser system. The system is hoped to reach sensitivities in the order of the Eötvös ($1E=10^{-9}s^{-2}$), which means that it would be capable of resolving a $10\times 10\times 10\text{cm}$ void at a depth of 1m. Published literature reports laboratory systems with gravity-gradient sensitivity of $4\text{ E/Hz}^{1/2}$ and accuracy of better than 1 E^{26} .

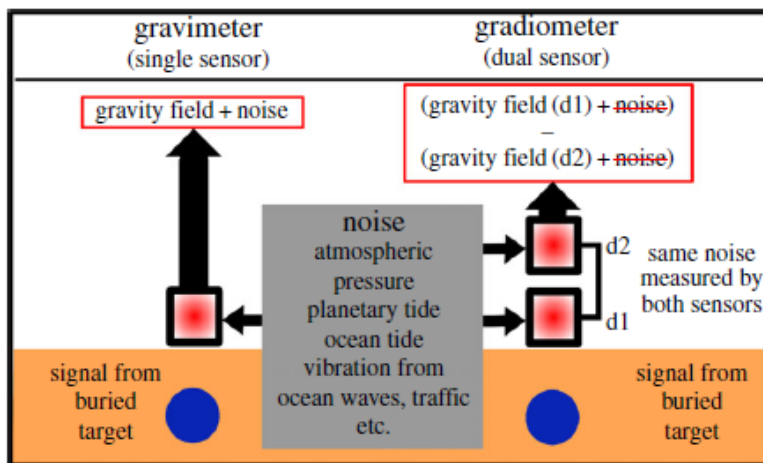


Fig. 27: Gravity gradiometer under development at Birmingham University²⁷.

Although CAI gravimeters based on atomic chips with Bose-Einstein condensates have not yet reached the stage of field deployability, we here give an example of the research status reporting some results by Rasel's group, see Fig. 28. They note that interferometers based on laser-cooled atoms are now commercially available as gravimeters with accuracy better than one part in 10^8 of gravity (corresponding to $10\mu\text{Gal}$), but Bose-Einstein condensates promise to improve these achievements and reach accuracies below a μGal . They demonstrate a quantum gravimeter based on an atom chip for the generation, delta-kick collimation, and coherent manipulation of a freely falling Bose-Einstein condensate, exploiting a launch mechanism based on Bloch oscillations and double Bragg diffraction. The chip-based gravimeter is shown in Fig. 26 (a), together with the space-time trajectories of a BEC without (b) and with (c) relaunch. The chip serves in all steps of state preparation and as retroreflector for light propagating in the z direction, thus creating moving lattices, which induce Bragg diffraction or Bloch oscillations for interferometry with BECs. The chip-scale BEC interferometer guarantees a free fall of tens of milliseconds in a volume as little as a one centimetre cube, and according to the authors paves the way for measurements with sub- μGal accuracies in miniaturized, robust devices.

²⁶ "Sensitive absolute-gravity gradiometry using atom interferometry", J. M. McGuirk et al., Phys. Rev. A 65, 033608, 2002; <https://journals.aps.org/prabstract/10.1103/PhysRevA.65.033608>

²⁷ "Development of a Transportable Cold Atom Gradiometer", Andrew Hinton, University of Birmingham, Thesis for the degree of Doctor of Philosophy, <https://etheses.bham.ac.uk/id/eprint/7120/1/Hinton16PhD.pdf>

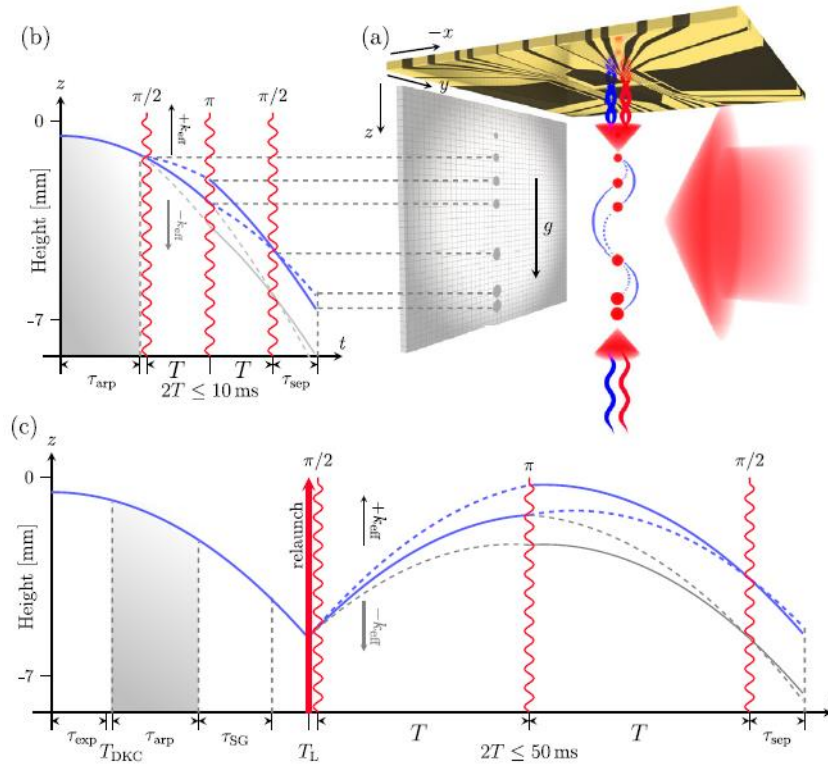


Fig. 28: Atom-chip fountain gravimeter²⁸.

We add here some general notes on the status of research on chip-scale atomic interferometry²⁹. In principle, confining cold atoms on a waveguide would allow both long interrogation time and compactness, so that chip-scale devices seem to be perfectly suited to provide the right performance mix for a wide range of applications. Until now, however, several technological issues prevented the experimental demonstration of a fully integrated chip-scale atomic interferometer with metrological capabilities.

Diverse techniques are being employed to split the atomic wavefunction in an atomic chip, including both optical transition, usually via Bragg scattering, and magnetic transitions, which typically exploit magnetic field gradients of RF pulses. Magnetic gradients and RF fields can be generated by feeding current to on-chip wires: it is indeed possible to micro-fabricate on an atom chip a complex wire pattern to create a sub-micrometric magnetic potential with the shape required for the targeted application. Very precise atomic position at the interferometer entrance can thus be ensured. Increase interrogation time can be obtained by trapping atoms in optical lattices and measuring the Bloch oscillations, instead of the free-falling or atomic fountain geometries which typically require more space. Measurement at the output is usually done outside the chip via absorption imaging, but the integration of optical elements on the atomic chip is also being investigated to enable more complex measurement schemes. Propagation of guided atoms in magnetic waveguides with relatively low currents (below hundreds of mA) can be obtained if the atoms are confined close to the chip surface. The coherent properties of the atomic states are however dramatically affected by surface corrugation, and fabrication defects still represent a fundamental limitation for atom chips. Indeed, surface roughness destroys system coherence and hinders atomic propagation (e.g by

²⁸ "Atom-Chip Fountain Gravimeter", S. Abend et al., Phys. Rev. Lett. 117, 203003, 2016; <https://journals.aps.org/prl/abstract/10.1103/PhysRevLett.117.203003>

²⁹ "Fifteen years of cold matter on the atom chip: promise, realizations, and prospects", Mark Keil, Omer Amit, Shuyu Zhou, David Groswasser, Yonathan Japha, and Ron Folman, Journal of Modern Optics, Vol. 63, N. 18, 1840-1885, 2016; <https://doi.org/10.1080/09500340.2016.1178820>

introducing cloud fragmentation), therefore limiting the interrogation time. Guiding the atoms far from the surfaces would attenuate these disturbances, but at the cost of higher currents, which means high power consumption and heating of in-chip wires. The manufacturing of the wires is also a very sensitive issue, since wire defects gives rise to fluctuations in the magnetic fields which are used to control the atoms and therefore constitutes an additional noise source. Several microfabrication techniques exist, with different cost and performances: for example metal evaporation produces smooth surfaces, but is not suitable for mass production, while metallization trough electroplating can be considered a good compromise for several applications. In addition to microfabrication, several enabling technologies need to be further developed in order to achieve chip-scale CAI sensors capable of metrological performances: mostly mentioned in this respect are dynamic vacuum systems capable of very rapid switching from high to low pressure, low noise current sources, and low-noise lasers.

As already stated, cold atom interferometry is a well-established instrument for scientific investigations. To give some examples of large-scale CAI infrastructure aimed at fundamental physics experiments, we mention the ~ 8 meter drop tower in Stanford, where cold atom-based gravity sensing has achieved the most precise measurement of local gravity to date, i.e. $6.7 \times 10^{-12} \text{ g}$ ³⁰. A scheme of the apparatus and its main characteristics is provided in Fig. 29.

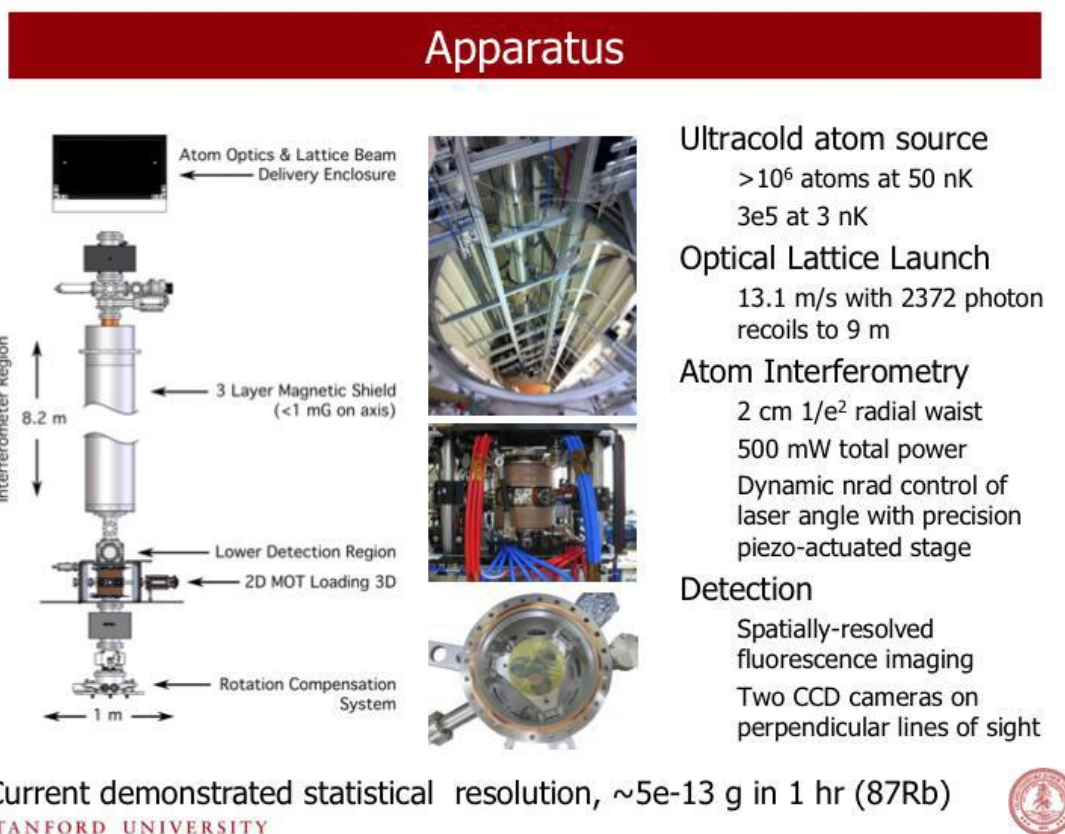


Fig. 29: Stanford drop tower for CAI gravimetry; with an interrogation time of $2T = 2.3$ seconds a resolution of $6.7 \times 10^{-12} \text{ g/shot}$ has been demonstrated³¹

³⁰ "Multiaxis inertial sensing with long-time point source atom interferometry", S.M. Dickerson et al., Phys. Rev. Lett., Vol. 111, N. 083001, 2013; <https://journals.aps.org/prl/abstract/10.1103/PhysRevLett.111.083001>

³¹ <https://slideplayer.com/slide/4665984/>; <http://web.stanford.edu/group/kasevich/cgi-bin/wordpress/wp-content/uploads/2014/10/sugarbakerThesis-augmented.pdf>

According to available information, a 10-meter drop tower for CAI gravimetry is also being built in Wuhan³². Close to Wuhan is under development the underground Zhaoshan long-baseline Atom Interferometer Gravitation Antenna (ZAIGA). As shown in Fig. 30, ZAIGA is configured as an equilateral triangle with two 1-km-apart atom interferometers in each arm, a 300-meter vertical tunnel with an atom fountain and atom clocks, and a tracking-and-ranging 1-km-arm-length prototype with lattice optical clocks linked by locked lasers. Long-baseline atom interferometers, high-precision atom clocks, and large-scale gyros will be used for experimental research on gravitation problems, such as gravitational wave detection, high-precision test of the equivalence principle, clock-based gravitational red-shift measurement, rotation measurement and gravito-magnetic effect.



Fig. 30: ZAIGA layout³³.

In Europe, the MIGA (Matter Wave laser Interferometric Gravitation Antenna) project is being funded by the French National Research Agency. It will be used both to monitor the evolution of the Earth gravitational field and to detect gravitational waves. The experiment will be realized at the underground facility of the Laboratoire Souterrain à Bas Bruit (LSBB) in Rustrel, and is composed by an hybrid atom-laser antenna which will make use of several atom interferometers simultaneously interrogated by the resonant mode of an optical cavity, see Fig. 31.

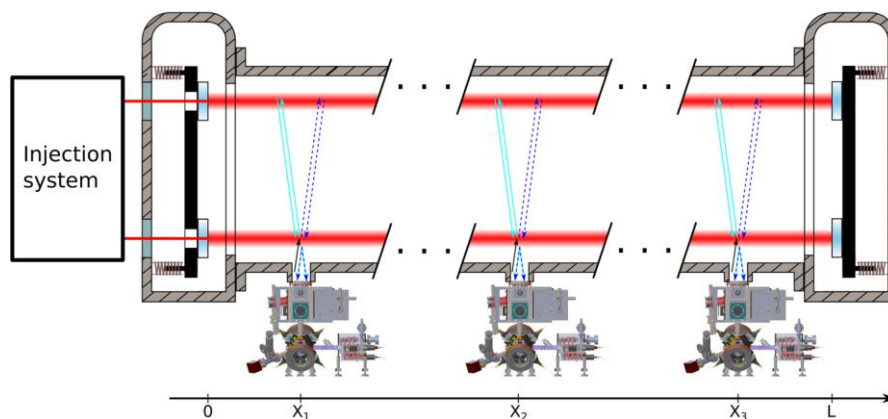


Fig. 31: MIGA measurement principle³⁴.

³² "Development of an atom gravimeter and status of the 10-meter atom interferometer for precision gravity measurement", L. Zhou et al., *General Relativity and Gravitation*, N. 43, 1931–1942, 2011; <https://link.springer.com/article/10.1007/s10714-011-1167-9>

³³ "ZAIGA: Zhaoshan long-baseline atom interferometer gravitation antenna", Ming-Sheng Zhan et al., *International Journal of Modern Physics D*, Vol. 29, No. 04, 1940005, 2020; <https://www.worldscientific.com/doi/10.1142/S0218271819400054>

³⁴ "Exploring gravity with the MIGA large scale atom interferometer", B. Canuel, et al., *Scientific Reports*, Vol. 8, N. 14064, 2018; <https://www.nature.com/articles/s41598-018-32165-z>

4 Worldwide players

We report in Table 1 a list of the main groups working on cold atom interferometry.

Country	Institution	PI	Topics/Expertise	Atom/Techniques	Link
France	SYRTE, Paris	Landragin, Pereira	gravimetry, gyroscope, gradiometer, GW detection	Rb, Cs	website
France	LKB, Paris	Guellati, Cladé	LMT, Bloch oscillations	Rb	website
France	ONERA, Palaiseau	Zahzam, Bidel	gravimetry, gradiometry, field applications	Rb	website
France	iXBlue/IOGS, Bordeaux	Barrett, Bouyer	inertial sensors	Rb	website
France	Muquans (company), Bordeaux	B. Desruelle (CEO)	gravimeter, gradiometer	Rb	website
France	Thales Group (company), Palaiseau	-	accelerometer, atom chip	Rb	article
France	LP2N, Bordeaux	Bouyer, Canuel	EP, GW	Rb, Sr	website
France	LCAR, Toulouse Univ.	Vigué, Gauguier	atom chips, atomic beams, cold atoms	Li, Rb	website
Germany	Hannover Univ.	Rasel	gravimeter, gradiometer, EP, GW, LMT	Rb, Yb	website
Germany	Humboldt Univ.	Peters, Krutzik	gravimetry, EP	Rb	website
Greece	IESL-FORTH, Crete	von Klitzing	guided interferometry, BEC	Rb	website
Italy	LENS, Florence	Tino, Poli	gradiometry, trapped atom interferometry	Rb, Sr, Cd	website
Italy	AtomSensors (company)	-	gravimeter, gradiometer	Rb	website
UK	Univ. Birmingham	Bongs	gravimeters, gradiometers, towards field applications	Rb	website
UK	Imperial College London	Hinds	accelerometry	Rb	website
UK	Univ. Nottingham	Fernholtz	guided interferometry	Rb	website
UK	Teledyne e2V (company)	-	gravimetry	Rb	website
UK	M2 lasers (company)	-	accelerometer	Rb	website
USA	Stanford	Kasevich, Hogan	EP, GW detection, LMT, BEC	Rb, Sr, 10-meter fountain	website
USA	Berkeley	Mueller	tests of fundamental physics, LMT	Cs	website
USA	JPL	Yu	applications in geodesy, gradiometry	Rb	website
USA	Sandia National Lab.	Biederman	high sampling rates, vapor cell, multi-axis		website

USA	Cambridge	Stoner	LMT, BEC		article
USA	Univ. Washington	Gupta	LMT, BEC		website
USA	AO Sense (company)	B. Young (CEO)	gravimetry, inertial sensors		website
USA	ColdQuanta (company)	Robert Ewald (CEO)	Ultra-cold- and cold-atom systems; chips		website
USA	NIST	Kitching, Donley	miniature AI for inertial sensing	Rb	website
USA	Northwestern Univ.	Kovatchy	GW, LMT		website
USA	Goddard (NASA)	Saif	gradiometry		article
Mexico	Univ. San Lui Potosi	Gomez, Franco	gravimeter	Rb	website
Australia	ANU	J. Close, N. Robins	gravimeter, gradiometer, LMT, BEC	Rb	website
China	Wuhan Institute of Physics	M. Zhan	gravimeter, EP, GW	Rb, Sr, Cs, 10-meter fountain	website
China	Zhejiang Univ. of Technology	Q. Lin	gravimetry	Rb	article
China	HUST, Wuhan	Zhong-Kun Hu	gravimetry, EP	Rb	website
China	National Institute of Metrology, Beijing	Shao-Kai Wang	gravimetry	Rb	article
China	National Laboratory Shanghai	Shuai Chen	gravimetry	Rb	website
China	Beihang University	Jian-Cheng Fang	Inertial navigation		website
Korea	KRISS	Dai-Hyuk Yu	gravimeter	Rb	article
India	IISER Pune	Krishnakumar	AI with BEC	Rb	website
Israel	Weizman Institue	Davidson, Firstenberg	gravimeter, inertial navigation	Rb	website
Japan	Univ. Tokyo	Katori	optically guided interferometry	Sr	article
New Zealand	Univ. Otago	Andersen	gravimeter	Rb	website
Singapore	CQT	Dumcke	portable gravimeter	Rb	website
Singapore	NTU	S.-Y. Lan	hollow core fiber AI	Rb	website
Singapore	Atomionics (company)	-	inertial sensors for navigation	-	website

Table 1: main research groups working on cold atom interferometry. EP: Equivalence Principle; GW: Gravitational Wave; LMT: Large Momentum Transfer techniques; BEC: Bose Einstein Condensates.

The above Table 1 has been taken from Geiger’s “Habilitation à Diriger des Recherches”³⁵, and completed to the best of our knowledge.

An idea of the main themes being pursued by the scientific community (at least in Europe) can be gathered from the COST action Quantum Technologies with Ultra-Cold Atoms, AtomQT, which mission is “the creation of a large network of expert groups on cold-atom quantum physics that will act as a catalyst in the rapid development and commercialization of quantum technology based on ultra-cold atoms and Bose-Einstein condensates”³⁶.

Other stakeholders can be deduced from a patent analysis on cold atom interferometry published in 2019. It lists ~150 application families (as per 2016), with a clear increasing trend driven by patents filed by Chinese players, see Fig. 32. Patents cover both technology developments (new design for magnetic traps, atomic chips, beam control, etc.) and possible applications. Among them, by far the most common are gravity sensors and devices to be used for positioning and navigation. Clocks enter in this analysis only tangentially, since, although they can make use of cold atoms, they usually do not exploit matter interferometry.

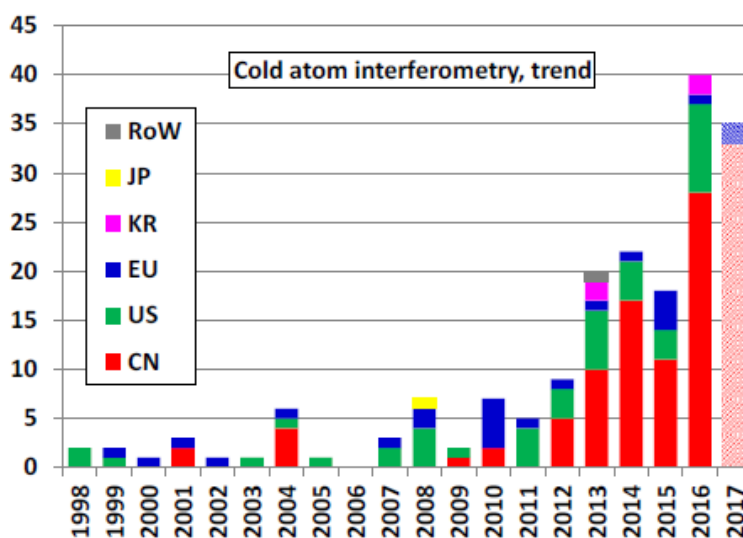


Fig. 32: time evolution of patent applications on cold atom interferometry³⁷.

Most of the applicants are universities, but there are also some dedicated start-ups (Aosense, Muquans, Coldquanta), national laboratories (Sandia from US, 717th Research Institute and Flight Automatic Control research Institute from China, CNRS from France), and some large corporations – especially from the defence sector. In particular the following defence players are note of mention:

- National University for Defense Technology of the People Liberation Army (China)
- Defense Agency (South Korea)
- US Navy and Air force / Charles Draper Labs / Honeywell / Northrop Grumman / Lockheed Martin (US)
- Onera / Thales / Sagem – Safran (FR)

³⁵ “Atom interferometry: from fundamental physics to precision inertial measurements”, Habilitation à Diriger des Recherches, Remi Geiger, Sorbonne Université and Systèmes de Référence Temps-Espace, 2019; <https://tel.archives-ouvertes.fr/tel-02267800/document>

³⁶ <https://atomqt.eu/>

³⁷ “Patent analysis of selected quantum technologies”, M. Travagnin, JRC Technical Report, EUR 29614EN, 2019; <https://ec.europa.eu/jrc/en/publication/patent-analysis-selected-quantum-technologies>

5 Conclusions

Inertial and gravity sensors based on Cold Atom Interferometry are already employed in laboratories or in controlled environments as very precise customized absolute measurement instruments, to address fundamental physics questions or metrological problems. Transportable gravimeters are also becoming available, and are starting to prove their usefulness as absolute instrument both for geophysics applications and for gravity surveys. Proof-of-principle demonstrations have also been made for CAI-based inertial sensors to be used for autonomous navigation.

According to a possible vision³⁸, the next application stage for inertial sensors and gravimeters will be space, where they can take advantage of the longer interrogation time and thus of the increased sensitivity enabled by microgravity. Scientific programmes for fundamental physics measurements based on CAI sensing in space are underway, and the possibly to exploit them for earth observation is being discussed. Indeed, experiments with Bose-Einstein condensates generated in chip-scale devices have already been performed in the ISS. However, reaching the level of integration and metrological capabilities necessary for actual applications (e.g. satellite-based gravimetry) still requires substantial technology development³⁹. On Earth, building robust gravimeters or gravity gradiometers capable of operating in mobile platforms will enable applications in civil engineering, and in oil and mineral prospecting. As a final step, the development of high bandwidth gyroscopes and accelerometers will allow using CAI inertial sensors for high-end autonomous navigation.

To accompany the technological evolution of CAI sensors towards applications, long-term policies are necessary which ensure continuous support. Ideally, programmes must be devised and implemented which foster fundamental and applied physics research, progress in enabling technologies, development of prototypes and early adoption. In particular, devices based on ultra-cold Bose-Einstein condensates are at a lower stage of application readiness, and require a better understanding of the phenomena setting their ultimate limits. Several key components have been identified whose development is critical for the technological advancement of CAI. Among them, we can highlight compact atomic physics chambers, fast vacuum switching systems, lasers with low phase noise, integrated optical modulators, low-weight isolators and polarizers, fibre optics components, detectors, auxiliary sensors, electronics for control and computation. To advance chip-scale systems, low-noise current generators and especially microfabrication capabilities can be added to this wish-list; the integration of functions which are currently realized off-chip (typically, the detection stage) must also be targeted. New algorithms with increased signal processing capability must also be devised, in order to take advantage of the exquisite sensitivity of these devices by filtering out noise without the necessity of longer averaging intervals.

All in all, although some niche applications are already starting to materialize, the path towards a full realization of the potentials of cold atom interferometry is still long. Longer still is the path to have fully-integrated chip-scale devices exploiting the properties of ultra-cold Bose-Einstein condensates. However, the present state of the art and the continuous progress being made is maybe calling for something more than the “broadband” long-term support initiatives detailed above. Scientists and policymakers should jointly identify a targeted application in an area of strategic EU interest, to engage in a medium-term technology demonstration. As an example, the challenges posed by a scientific space mission could catalyse the potentials available in the EU research community, and encourage it to work with industry to advance and actually prove in the field the capabilities of sensors based on cold atom interferometry.

³⁸ “Taking atom interferometric quantum sensors from the laboratory to real-world applications”, K. Bongs et al., *Nature Reviews Physics*, Vol. 1, Pg. 731–739, 2019; <https://www.nature.com/articles/s42254-019-0117-4>

³⁹ “ESA’s next-generation gravity mission concepts”, R. Haagmans et al., *Rend. Fis. Acc. Lincei*, 2020; <https://doi.org/10.1007/s12210-020-00875-0>

References

- [1] "Mobile and remote inertial sensing with atom interferometers", B. Barrett et al., Proc. International School of Physics 'Enrico Fermi', 188, 493-555, 2014; <https://arxiv.org/pdf/1311.7033.pdf>
- [2] "Experimental gravitation and geophysics with matter wave sensors", P. Bouyer, Frontier of matter-wave optics conference, 2018; <https://www.matterwaveoptics.eu/FOMO2018/school/lecture-notes/Bouyer%20--%20experimental%20gravitation%20and%20geophysics%20with%20matterwave%20sensors.pdf>
- [3] "Fifteen years of cold matter on the atom chip: promise, realizations, and prospects", Mark Keil et al., Journal of Modern Optics, Vol. 63, N. 18, 1840-1885, 2016; <https://doi.org/10.1080/09500340.2016.1178820>
- [4] "Measurement of the gravitational acceleration of an atom with a light-pulse atom interferometer", M. Kasevich et al., Applied Physics B, Vol. 54, 321-332, 1992; <https://link.springer.com/article/10.1007/BF00325375>
- [5] "Long-Term Stability of an Area-Reversible Atom-Interferometer Sagnac Gyroscope", D. S. Durfee et al., Phys. Rev. Lett. 97, 240801, 2006; <https://arxiv.org/pdf/quant-ph/0510215.pdf>
<https://journals.aps.org/prl/abstract/10.1103/PhysRevLett.97.240801>
- [6] "Six-Axis Inertial Sensor Using Cold-Atom Interferometry", B. Canuel et al., Phys. Rev. Lett. 97, 010402, 2006; <https://journals.aps.org/prl/abstract/10.1103/PhysRevLett.97.010402>
<https://arxiv.org/pdf/physics/0604061.pdf>
- [7] "Detecting inertial effects with airborne matter-wave interferometry", R. Geiger et al., Nature Communications Vol. 2, N. 474, 2011; <https://www.nature.com/articles/ncomms1479>
- [8] "A compact dual atom interferometer gyroscope based on laser-cooled rubidium", T. Müller et al., The European Physical Journal D, Vol. 53, 273-281, 2009; <https://link.springer.com/article/10.1140/epjd/e2009-00139-0>
- [9] "Dual-Axis High-Data-Rate Atom Interferometer via Cold Ensemble Exchange", Akash V. Rakholia et al., Physical Review Applied, Vol. 2, N. 054012, 2014; <https://arxiv.org/pdf/1407.3847.pdf>
<https://journals.aps.org/prapplied/abstract/10.1103/PhysRevApplied.2.054012>
- [10] "Hybridizing matter-wave and classical accelerometers", J. Lautier et al., Appl. Phys. Lett. Vol. 105, No. 144102, 2014, <https://aip.scitation.org/doi/pdf/10.1063/1.4897358>; <https://arxiv.org/pdf/1410.0050.pdf>
- [11] "Composite-Light-Pulse Technique for High-Precision Atom Interferometry", P. Berg et al., Phys. Rev. Lett. Vol. 114, No. 063002, 2015; <https://journals.aps.org/prl/abstract/10.1103/PhysRevLett.114.063002>
- [12] "Dual matter-wave inertial sensors in weightlessness", Brynle Barrett et al., Nature Communications, Vol. 7 N. 13786, 2016; <https://www.nature.com/articles/ncomms13786>
- [13] "Interleaved atom interferometry for high-sensitivity inertial measurements", D. Savoie et al., Science Advances, Vol. 4, N. 12, 2018; <https://advances.sciencemaq.org/content/4/12/eaau7948>
<https://arxiv.org/pdf/1808.10801.pdf>
- [14] "Navigation-compatible hybrid quantum accelerometer using a Kalman filter", P. Cheiney et al., Physical Review Applied Vol. 10, N. 034030, 2018; <https://arxiv.org/pdf/1805.06198.pdf>
<https://journals.aps.org/prapplied/abstract/10.1103/PhysRevApplied.10.034030>;
See also "Development of a compact cold atom sensor for inertial navigation", SPIE Photonics Europe (Brussels), 2016, published in Quantum Optics, Vol. 9900 (2016) <https://doi.org/10.1117/12.2228351>
- [15] "Single-Source Multiaxis Cold-Atom Interferometer in a Centimeter-Scale Cell", Yun-Jih Chen et al., Physical Review Applied, Vol. 12, N. 014019, 2019; <https://arxiv.org/abs/1812.00106>
<https://journals.aps.org/prapplied/abstract/10.1103/PhysRevApplied.12.014019>
- [16] "Gravity surveys using a mobile atom interferometer", Xuejian Wu et al., Science Advances, Vol. 5, no. 9, 2019, <https://advances.sciencemaq.org/content/5/9/eaax0800>
- [17] "Gravity measurements below $10^{-9}g$ with a transportable absolute quantum gravimeter", V. Ménot et al., Scientific Reports, Vol. 8, 12300, 2018, <https://www.nature.com/articles/s41598-018-30608-1.pdf>
- [18] "Mobile quantum gravity sensor with unprecedented stability", C. Freier et al., 8th Symposium on Frequency Standards and Metrology, Journal of Physics: Conference Series 723, 012050, 2016
<https://iopscience.iop.org/article/10.1088/1742-6596/723/1/012050>

- [19] "Micro-Gal level gravity measurements with cold atom interferometry", Zhou Min-Kang et al., Chinese Physics B, Vol. 24, N. 5, 2015; <https://iopscience.iop.org/article/10.1088/1674-1056/24/5/050401>
- [20] "Operating an atom-interferometry-based gravity gradiometer by the dual-fringe-locking method", Xiao-Chun Duan et al., Phys. Rev. A 90, 023617, 2014; <https://journals.aps.org/pr/abstract/10.1103/PhysRevA.90.023617>
- [21] "Compact portable laser system for mobile cold atom gravimeters", Xiaowei Zhang et al., Applied Optics, Vol. 57, Issue 22, 2018; <https://www.osapublishing.org/ao/abstract.cfm?uri=ao-57-22-6545>
- [22] "Absolute airborne gravimetry with a cold atom sensor", Yannick Bidet et al., Journal of Geodesy Vol. 94, N. 20, 2020; <https://link.springer.com/article/10.1007/s00190-020-01350-2>
<https://arxiv.org/pdf/1910.06666.pdf>
- [23] "Absolute marine gravimetry with matter-wave interferometry", Y. Bidet et al., Nature Communications Vol. 9, 627, 2018; <https://www.nature.com/articles/s41467-018-03040-2>
- [24] "A portable magneto-optical trap with prospects for atom interferometry in civil engineering" A. Hinton et al., Philos Trans A Math Phys Eng Sci. 375(2099), 2017; <https://royalsocietypublishing.org/doi/10.1098/rsta.2016.0238>
- [25] <http://assessingtheunderworld.org/wp-content/uploads/2016/05/12086-GG-Tops-brochure-Final.pdf>
- [26] "Development of a Transportable Cold Atom Gradiometer", Andrew Hinton, University of Birmingham, Thesis for the degree of Doctor of Philosophy, <https://etheses.bham.ac.uk/id/eprint/7120/1/Hinton16PhD.pdf>
- [27] "Sensitive absolute-gravity gradiometry using atom interferometry", J. M. McGuirk et al., Phys. Rev. A 65, 033608, 2002; <https://journals.aps.org/pr/abstract/10.1103/PhysRevA.65.033608>
- [28] "Atom-Chip Fountain Gravimeter", S. Abend et al., Phys. Rev. Lett. 117, 203003, 2016; <https://journals.aps.org/prl/abstract/10.1103/PhysRevLett.117.203003>
- [29] "Fifteen years of cold matter on the atom chip: promise, realizations, and prospects", Mark Keil, Omer Amit, Shuyu Zhou, David Groswasser, Yonathan Japha, and Ron Folman, Journal of Modern Optics, Vol. 63, N. 18, 1840-1885, 2016; <https://doi.org/10.1080/09500340.2016.1178820>
- [30] "Multi-axis inertial sensing with long-time point source atom interferometry", S.M. Dickerson et al., Phys. Rev. Lett., Vol. 111, N. 083001, 2013; <https://journals.aps.org/prl/abstract/10.1103/PhysRevLett.111.083001>
- [31] <https://slideplayer.com/slide/4665984/>; <http://web.stanford.edu/group/kasevich/cqi-bin/wordpress/wp-content/uploads/2014/10/sugarbakerThesis-augmented.pdf>;
- [32] "Development of an atom gravimeter and status of the 10-meter atom interferometer for precision gravity measurement", L. Zhou et al., General Relativity and Gravitation, N. 43, 1931-1942, 2011; <https://link.springer.com/article/10.1007/s10714-011-1167-9>
- [33] "ZAIGA: Zhaoshan long-baseline atom interferometer gravitation antenna", Ming-Sheng Zhan et al., International Journal of Modern Physics D, Vol. 29, No. 04, 1940005, 2020; <https://www.worldscientific.com/doi/10.1142/S0218271819400054>
- [34] "Exploring gravity with the MIGA large scale atom interferometer", B. Canuel, et al., Scientific Reports, Vol. 8, N. 14064, 2018; <https://www.nature.com/articles/s41598-018-32165-z>
- [35] "Atom interferometry: from fundamental physics to precision inertial measurements", Habilitation à Diriger des Recherches, Remi Geiger, Sorbonne Université and Systèmes de Référence Temps-Espace, 2019; <https://tel.archives-ouvertes.fr/tel-02267800/document>
- [36] <https://atomqt.eu/>
- [37] "Patent analysis of selected quantum technologies", M. Travagnin, JRC Technical Report, EUR 29614EN, 2019; <https://ec.europa.eu/jrc/en/publication/patent-analysis-selected-quantum-technologies>
- [38] "Taking atom interferometric quantum sensors from the laboratory to real-world applications", K. Bongs et al., Nature Reviews Physics, Vol. 1, Pg. 731-739, 2019; <https://www.nature.com/articles/s42254-019-0117-4>
- [39] "ESA's next-generation gravity mission concepts", R. Haagmans et al., Rend. Fis. Acc. Lincei, 2020; <https://doi.org/10.1007/s12210-020-00875-0>

List of abbreviations and definitions

BEC: Bose-Einstein Condensate

CAI: Cold Atom Interferometry

DARPA: Defense Advanced Research Projects Agency (USA)

DGA: Direction générale de l'armement (Ministère des Armées, France)

DTRA: Defense Threat Reduction Agency (USA)

DTU Space: Danmarks Tekniske Universitet - Denmark's National Space Institute

ESA: European Space Agency

EP: Equivalence Principle

FCCG: Falling Corner Cube Gravimeter

GW: Gravitational Wave

ICAG: International Comparison of Absolute Gravimeters

IMU: Inertial Measurement Unit

LMT: Large Momentum Transfer

MIGA: Matter wave laser based Interferometer Gravitation Antenna

MOT: Magneto Optical Trap

MZI: Mach-Zehnder Interferometer

NASA: National Aeronautics and Space Administration (USA)

NSF: National Science Foundation (USA)

ONERA: Office National d'Etudes et de Recherches Aérospatiales (France)

PSI: Point-Source Interferometry

RF: Radio Frequency

SCG: Superconducting Gravimeter

SCI: Symmetrized Composite-pulse Interferometer

SYRTE: Systèmes de Référence Temps-Espace (France)

UFF: Universality of Free Fall

GETTING IN TOUCH WITH THE EU

In person

All over the European Union there are hundreds of Europe Direct information centres. You can find the address of the centre nearest you at: https://europa.eu/european-union/contact_en

On the phone or by email

Europe Direct is a service that answers your questions about the European Union. You can contact this service:

- by freephone: 00 800 6 7 8 9 10 11 (certain operators may charge for these calls),
- at the following standard number: +32 22999696, or
- by electronic mail via: https://europa.eu/european-union/contact_en

FINDING INFORMATION ABOUT THE EU

Online

Information about the European Union in all the official languages of the EU is available on the Europa website at: https://europa.eu/european-union/index_en

EU publications

You can download or order free and priced EU publications from EU Bookshop at: <https://publications.europa.eu/en/publications>. Multiple copies of free publications may be obtained by contacting Europe Direct or your local information centre (see https://europa.eu/european-union/contact_en).

The European Commission's science and knowledge service

Joint Research Centre

JRC Mission

As the science and knowledge service of the European Commission, the Joint Research Centre's mission is to support EU policies with independent evidence throughout the whole policy cycle.



EU Science Hub

ec.europa.eu/jrc



@EU_ScienceHub



EU Science Hub - Joint Research Centre



Joint Research Centre



EU Science Hub



Publications Office
of the European Union

doi:10.2760/315209

ISBN 978-92-76-20405-3